Journal of Inflammation Research Dovepress

Open Access Full Text Article ORIGINAL RESEARCH

Trimethylamine N-Oxide Aggravates Neuro-Inflammation via lncRNA Fendrr/miR-145-5p/PXN Axis in Vascular Dementia Rats

Yang Deng[1,*], Rui Duan[2,*], Ye Hong[2,*], Qiang Peng[2], Zhong-Yuan Li[2], Xiang-Liang Chen[2], Ying-Dong Zhang[1]

[1]Department of Neurology, Nanjing First Hospital, China Pharmaceutical University, Nanjing, 210006, People's Republic of China; [2]Department of Neurology, Nanjing First Hospital, Nanjing Medical University, Nanjing, 210006, People's Republic of China

*These authors contributed equally to this work

Correspondence: Xiang-Liang Chen, Department of Neurology, Nanjing First Hospital, Nanjing Medical University, No. 68, Changle Road, Nanjing, Jiangsu, 210006, People's Republic of China, Email chenxl@njmu.edu.cn; Ying-Dong Zhang, Department of Neurology, Nanjing First Hospital, China Pharmaceutical University, No.68, Changle Road, Nanjing, Jiangsu, 210006, People's Republic of China, Email zhangyingdong@njmu.edu.cn

Purpose: Vascular dementia (VaD) is the second most common dementia in the world. An increasing number of studies have demonstrated the important role of long non-coding RNAs (lncRNAs) in VaD. Our previous investigation demonstrated that Trimethylamine-N-oxide (TMAO) exacerbates cognitive impairment and neuropathological alterations in VaD rats. Thus, we hypothesized that TMAO could play an injury role in VaD by regulating lncRNAs.

Materials and Methods: The rats using the bilateral common carotid artery (2VO) model were administered TMAO (120 mg/kg) for 8 consecutive weeks, 4 weeks preoperatively and 4 weeks postoperatively. High-throughput sequencing was conducted to investigate the effects of TMAO treatment on lncRNA expression in rat hippocampus and bioinformatics analysis was performed to identify potential downstream targets. Reverse transcription-quantitative polymerase chain reaction (RT-qPCR) was used to detect the levels of lncRNA fetal-lethal noncoding developmental regulatory RNA (Fendrr), miR-145-5p, and paxillin (PXN). Learning and spatial memory capacities were measured, as well as inflammatory factors. Nissl staining was used to observe neuronal injury in the CA1 area of the hippocampus. Furthermore, we used the Fendrr loss-of-function assay, miR-145-5p gain-of-function assays and PXN loss-of-function assay to explore the mechanisms by which TMAO acts on VaD.

Results: TMAO administration upregulated lncRNA Fendrr expression in the rat hippocampus, while the damaging effects of TMAO were counteracted after knockdown of Fendrr. Fendrr exhibits highly expressed in 2VO rats and sponged miR-145-5p, which targets PXN. Silencing of Fendrr or PXN, or promotion of miR-145-5p improved neurological function injury, reduced neuronal damage, as well as repressed inflammation response. Inhibition of miR-145-5p abrogated up Fendrr knockdown mediated influence on 2VO rats.

Conclusion: The results of this study indicated that TMAO inhibits the miR-145-5p/PXN axis by increasing the Fendrr expression, thus exacerbating the development of VaD.

Keywords: trimethylamine N-oxide, neuroinflammation, Fendrr, MiR-145-5p, PXN, vascular dementia

Introduction

Vascular dementia (VaD) is characterized by the loss of cognitive function caused by cerebrovascular and cardiovascular pathologic changes, mainly manifested as learning and memory dysfunction.[1] It has a poor prognosis, with a 5-year mortality rate of 61%, significantly higher than most dementia types.[2] The available therapeutic agents for VaD are cholinesterase inhibitors, but these drugs may cause a large range of adverse events, including headache, joint pain and gastrointestinal reactions, etc.,[3] while whether they can improve the patients is uncertain. Meanwhile, previous studies have found that several regulatory mechanisms participate in the pathologic process of VaD, including inflammation, apoptosis, and oxidative stress.[4,5] Therefore, there is an urgent need to further explore the pathological changes of VaD and the need for possible therapeutic targets.

Received: 18 July 2024
Accepted: 17 October 2024
Published: 21 October 2024

Recently, several studies have suggested that gut microbiota may be one of the major risk factors for VaD susceptibility.[6,7] A study by Liu et al was the first to show that vascular dementia is mediated by gut microbiota and its metabolites.[8] Trimethylamine N-oxide (TMAO) is a specialized metabolite processed by the intestinal microbiota. The intestinal microbiota processed certain ingested substances such as L-carnitine into trimethylamine (TMA), which is followed by transformation to TMAO via hepatic flavin monooxygenase 3 (FMO3) within the intestines.[9] Importantly, studies have displayed that higher circulating TMAO is associated with cognitive decline and dementia.[10,11] For instance, plasma concentrations of TMAO were positively related to NIHSS scores after stroke.[12] Gao et al stated that elevated plasma TMAO levels in APP/PS1 mice were correlated with worsening cognitive ability and AD pathology.[10] In addition, another study indicated that TMAO reduces antioxidant enzymes and accelerates brain aging by inducing neuronal aging, synaptic damage, and inhibiting the mTOR signaling pathway, leading to cognitive dysfunction.[13] Our previous study figured out that TMAO could impair cognitive function and activate the NLRP3 inflammasome in VaD rats.[14] However, the mechanism by which TMAO promotes VaD injury is currently unknown.

Long noncoding RNA (lncRNA) is a class of non-coding RNA with a length of more than 200 nucleotides, which plays an important role in almost every level of gene function and regulation.[15] Among them, lncRNA Fendrr has been described as involved in neural stem cells differentiation,[16] and neural stem cell-driven cell rejuvenation and/or repair enhances neural networks and improves cognitive performance.[17] Importantly, lncRNA Fendrr has recently been found to be strongly associated with cerebrovascular diseases. For instance, lncRNA Fendrr could upregulate VEGFA via miR-126, which promoted apoptosis of cerebral microvascular endothelial cells and thus exacerbated hypertensive intracerebral hemorrhage in mice.[18] Also, lncRNA Fendrr was observed to be involved in pyroptosis and inflammation of microglia in diabetes-cerebral ischemia/reperfusion (I/R) mice.[19] Nevertheless, the role of Fendrr in cognitive impairment and its effect on neuroinflammation in VaD have not yet been explored.

Multiple studies have cleared that lncRNA can act as a miRNA sponge to negatively regulate its expression, thereby regulating the expression of multiple downstream mRNAs.[20–22] Through database prediction, we found that miR-145-5p is a potential binding target of Fendrr, and miR-145-5p has been recorded to be downregulated in multiple brain regions of VaD-related rodent models.[23] More importantly, miR-145-5p expression is associated with inflammatory response after ischemic injury.[24,25] The above studies suggest that miR-145-5p may be associated with VaD neuroinflammation. A previous study have indicated that miR-145-5p targets the paxillin (PXN) gene.[26] PXN is a molecular adaptor protein located on human chromosome 12q24.31, which plays an important role in physiological processes such as nervous system development, embryonic development, and vascular development.[27] In addition, PXN is also involved in pathological processes such as oxidative stress, inflammation, and endothelial cell barrier dysfunction.[28,29] Remarkably, in a previous study, Zhao et al have demonstrated that PXN is upregulated in cortical tissues of 2VO rats.[23] However, the expression and function of PXN in the hippocampus of VaD have not been reported. Based on this, we propose a reasonable hypothesis that TMAO can promote neuroinflammation after VaD by regulating lncRNA Fendrr to sponge miR-145-5p targeting PXN.

Materials and Methods

Ethics Statement

All animal experiments were approved by the Animal Ethics Committee of Nanjing First Hospital (protocol number: DWSY-2104386) and were carried out according to the National Institutes of Health "Guidelines for Care and Use of the Laboratory Animals". All efforts were made to minimize the number of rats used and their suffering.

VaD Animal Model and Corresponding Treatment

Healthy adult male SD rats (8 weeks old; weight 280–300 g) were provided by the Model Animal Research Center of Nanjing University (Nanjing, China) and raised under a 12-h dark/light cycle, appropriate temperature, suitable humidity and ad libitum feed. 4% isoflurane anesthetized the rats before surgery. TMAO was administered and 2VO model was established following our previous research protocol.[14] In brief, The rats were anesthetized and bilateral common carotid arteries were isolated and ligated gently. The sham operation group performed the same procedure, but did not include

the ligating step. After surgery, all rats were given lidocaine (10%) applied locally to the incision, ketoprofen (10 mg/kg, twice a day for two days) for analgesia and intramuscular penicillin (for one week) to prevent infection. The 2VO rats were continuously administered TMAO before and after surgery, while the rats were instilled with sterile water in the sham group.

TMAO (catalog number: 317594, purity: 95%, CAS: 1184-78-7) was purchased from Sigma-Aldrich. The lentivirus vectors (LV-sh-Fendrr, agomir-145-5p, antagomir-145-5p, and LV-sh-PXN) and lentiviral vector negative control were supplied by GenePharma (Shanghai, China). As previously reported,[30] lentivirus vectors were injected into the CA1 area of hippocampus 7 days before 2VO surgery. First, the stereotaxic device fixed the anesthetized rats (RWD LifeScience, CA, USA). Injection axes were as flows with reference to bregma: mediolateral, ±3.2 mm; anteroposterior, −4.52 mm; dorsoventral −3.16 mm using coordinates under the surface of skull. Two microliters of lentiviral vector were injected into the hippocampal CA1 region using a 10 μL syringe (Hamilton). After the injection was over, the needle was held in place for a moment and then removed extremely slowly to prevent the solution from flowing back. After removal of the needle, the drill holes were closed with bone wax and the incisions were sutured to rehabilitate the rats. Figure 1 presents a schematic timeline of experiments.

LncRNA Sequencing

The Gene Denovo Biotechnology Co., Ltd (Guangzhou, China) provided the RNA-sequencing analysis. Total RNA was extracted from rat hippocampal tissue using the Trizol kit (Life Technologies, CA, USA) and the sample RNA quality was evaluated by a 2100 Bioanalyzer (Agilent Technologies, CA, USA). After removing the ribosomal RNA, the total RNA obtained was reverse-transcribed to cDNA and then quantified as well as pooled using the ABI StepOnePlus Real-Time PCR System (Life Technologies). Finally, we performed up-sequencing according to the PE150 mode of Illumina novaseq 6000. Raw reads containing splice or low-quality bases were filtered by fastp (version 0.18.0). Ribosomal RNA (rRNA) was removed using the comparison tool bowtie2, and clean reads of paired ends were compared to a reference genome (Rattus norvegicus Ensembl_release106) using HISAT2 (version 2.1.0). StringTie software was used to perform quantitative analysis of lncRNA. Genes differential expression analysis was performed by DESeq2 software. Parameter $|\log2(\text{Foldchange})| \geq 1$ and P-value < 0.05 were defined as significantly differentially expressed lncRNAs. The sequencing database is archived in GenBank (GSE249873).

Functional Enrichment Analysis

The predicted differentially expressed mRNAs were analyzed by Gene Ontology (GO) analyses and Kyoto Encyclopedia of Genes and Genomes (KEGG) pathway analysis using the R package clusterProfiler. The p-value of < 0.05 was deemed significant for statistical analysis.

Open Field Test (OFT)

Open Field Test (OFT) is a simple behavioral test experiment that reflects the autonomous and exploratory behavior of experimental animals in unfamiliar environments. The basic principle is to place rats in an unfamiliar, open environment and record their activities. Briefly, the rats were placed in the center of a square black box and were allowed to move freely. The camera connected to an Any-maze® tracker recorded and calculated (New Soft Information Technology Co.,

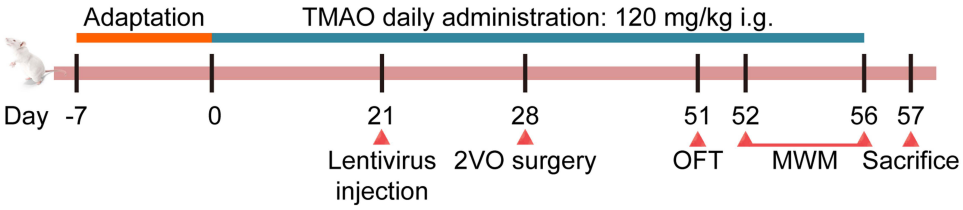

Figure 1 Schematic timeline of the animal study.
Abbreviations: OFT, Open Field Test; MWM, Morris Water Maze Test.

Ltd.™, Shanghai, China) the time spent by the rats and the total travel distance into the center. After each trial, the chamber was wiped with 75% ethanol and left to dry to avoid olfactory cues.

Morris Water Maze Test (MWM)

The water maze device, which is equally divided into four quadrants was employed and a transparent circular stage was under the water surface. Every rat was exposed to four training trials on 5 successive days. The rats were randomly put in the water from four quadrants each day until they found the stage and stayed for 15 s out of 60 s. When the stage was not found less than 60 s, the rats were brought into the stage. On the second day of the last trial, the path length of the rats to reach the stage was recorded by the video tracker (Noldus Information Technology B.V.™, Wageningen, Netherlands) after moving out of the stage, and the means of the four trials were determined.

Nissl Staining

Nissl staining was used to detect Nissl bodies in neurons. The paraffin-embedded brain tissues of rats were cut into 5 μm-thick sections, which were stained with Nissl staining solution for 1 h at 56 °C (Solarbio, Beijing, China) after dewaxing and rehydration. Next, the sections were dried with gradient concentrations of ethanol, rinsed with xylene, and sealed with neutral gum. Six fields of hippocampus were randomly selected on each coronal section using an Olympus microscope (Olympus™, Tokyo, Japan) for quantitative analysis. Nuclei with round cell bodies, cytoplasmic Nissl material and nucleoli visible were identified as normal neurons, whereas nuclei with disorganized arrangement, Nissl material disappearance, nuclei surrounded by voids and unrecognizable nucleoli were identified as damaged neurons. Nissl positive neurons % = positive neurons/total neurons ×100%.

Luciferase Report Assay

The wild-type (wt) or mutant-type (mut) 3′-UTRs of Fendrr or PXN were cloned into the pmirGLO vector (Promega, USA). HEK-293 T cells were seeded in 24-well plates. When the fusion reached 70–80%, cells were co-transfected with wt or mut 3′-UTRs of Fendrr or PXN luciferase reporter plasmids, together with agomir-NC or agomir-145-5p by Lipofectamine 2000. The cells were harvested 24 h after transfection, and assayed for luciferase activity.

Fluorescence in situ Hybridization (FISH)

FISH was applied to assay the localization of Fendrr, miR-145-5p and PXN expression in the sections of hippocampal tissue of 2VO rats with the FISH kit in accordance with the instructions of the manufacturer. In brief, the sections of paraffin-embedded hippocampus were soaked in xylene I (Guoyao, Shanghai, China) for 15 min, in xylene II for 15 min, and subsequently in pure ethanol (Guoyao, Shanghai, China) for 5 min. Then, the sections were digested with proteinase K (20 μg/mL, Servicebio, Wuhan, China) solution at 37°C for 25 min. For each section was added with the pre-hybridization solution (Riobo biotech, Guangzhou, China) for 1 h at 37°C. Hybridization buffer (Riobo biotech, Guangzhou, China) with 50 nM biotin-labeled lncFendrr (Gene Pharma, Shanghai, China) or miR-145-5p (Gene Pharma, Shanghai, China) was heated to 65 °C for 5 min and added dropwise to the sections, which were then allowed to hybridize at 37 °C overnight with or without anti-PXN (1:1000; #50195; CST; Boston, MA, USA). After washes and blocking, sections were incubated with DAPI (Servicebio, Wuhan, China) to stain the cell nuclei. The sections were observed with a Nikon upright fluorescence microscope (Nikon, Tokyo, Japan) and photographed. The sequence of the Fendrr probe was as follows: ATGTTCTAAATGTTTCTTGATTCTG; The sequence of the mir-145-5p probe was as follows: AGGGATTCCTGGGAAAACTGGAC.

RNA Immunoprecipitation (RIP) Assay

Ago2-RIP assays were carried out using an EZ-Magna RIP RNA kit (#17-704, Millipore, MA, USA). Hippocampal tissue was lysed in RIP lysis buffer and incubated with negative control IgG (Millipore, MA) or anti-Ago2 (#ab32381, Abcam) conjugated magnetic beads. Immunoprecipitated RNA was isolated by Proteinase K buffer and analyzed by RT-qPCR.

Reverse Transcription-Quantitative Polymerase Chain Reaction (RT-qPCR)

Total RNA of rat hippocampal tissues was isolated using Trizol reagent (Invitrogen, CA, USA). The obtained total RNA was reverse-transcribed to cDNA using the cDNA Synthesis Supermix kit (Takara, Japan). Then, the target genes were quantified with SYBR® Premix Ex TaqTM II (Takara, Japan) on the ABI 7500 fast real-time PCR system (Applied Biosystems, USA). The expression of target genes was analyzed by the $2^{-\Delta\Delta CT}$ method using U6 and β-actin as internal references for miRNA and mRNA, respectively. Primer sequences are listed in Supplemental Table S1.

Western Blot Analysis

Rat hippocampal tissues were homogenized with RIPA lysate buffer and the protein concentration was quantified with a BCA Protein Assay Kit (Thermo Fisher Scientific, Inc.™, Carlsbad, CA, USA). Equal amounts of samples were used to perform sodium dodecyl sulfate-polyacrylamide gel electrophoresis. The total protein was transferred to a polyvinylidene fluoride (PVDF) membrane (Millipore), which is blocked with 5% skimmed milk for 2 hours. PVDF membrane was incubated with anti-PXN (1:1000; #50195; CST; Boston, MA, USA) or β-actin (1:1000, #4970; CST, Boston, MA, USA), overnight at 4 °C, and anti-rabbit IgG HRP (1:4000; CST, Boston, MA, USA) for 2h at room temperature. The bands were finally visualized with the ECL kit (Millipore™, Merck, Darmstadt, Germany) and using the Image J to quantify the protein band density. All data were standardized to β-actin.

Enzyme-Linked Immunosorbent Assay (ELISA)

TNF-α, IL-1β and IL-6 ELISA kits (Abcam, MA, USA) were used in accordance with the manufacturer's instructions to evaluate the inflammatory cytokine levels in the hippocampus. The levels of these cytokines were measured by absorbance using a micro enzyme-linked immunosorbent assay reader (Tecan, USA).

Statistical Analysis

The experiment data were represented as the mean ± SD and analyzed by Prism 8 software (GraphPad™, San Diego, CA, USA). Comparison between the two groups was made using the *t*-test, and comparison among multiple groups was adopted using one-way or two-way analysis of variance (ANOVA) followed by Tukey's post-test. Each experiment was repeated at least 3 times. Data were deemed to be statistically significant when $P < 0.05$.

Results

TMAO Promoted Hippocampal Inflammatory Response Within 2VO Rats

To identify the role of TMAO treatment on function and signaling pathways in 2VO rats, we carried out GO enrichment analysis and KEGG signaling pathway analyses of the differential genes (DEGs) from transcriptome analysis. Figure 2A–C shows the top ten enriched GO terms. Biological processes are primarily associated with immune responses, defense responses, stimulus responses, and immune system processes. Most of the genes in cellular components are involved in the external side of plasma membrane and cell surface. Among the molecular functions, protein binding, immune receptor activity and receptor binding are significantly affected. The KEGG pathway analysis indicated that the DEGs were predominantly enriched in the B cell receptor signaling pathway, formation of neutrophil extracellular traps, NF-kappa B signaling pathway, Fc gamma R-mediated phagocytosis, and NOD-like receptor signaling pathway. Besides, other enrichment pathways involved the Toll-like receptor signaling pathway, the JAK-STAT signaling pathway and the PI3K-Akt signaling pathway (Figure 2D). These pathways have been confirmed to regulate cellular immunity and inflammatory responses.[31–33] Based on the above, we examined the levels of TNF-α, IL-1β and IL-6 in the hippocampus of TMAO-treated 2VO rats, and the results showed that TMAO treatment significantly increased the secretion of inflammatory factors in the 2VO rats hippocampus (Figure 2E–G).

TMAO Up-Regulates Hippocampal lncRNA Fendrr Expression in 2VO Rats

In order to explore the detailed mechanisms underlying the action of TMAO on 2VO rats, we performed high-throughput sequencing of hippocampus from 2VO rats and 2VO rats administered with TMAO. First, principal component analysis

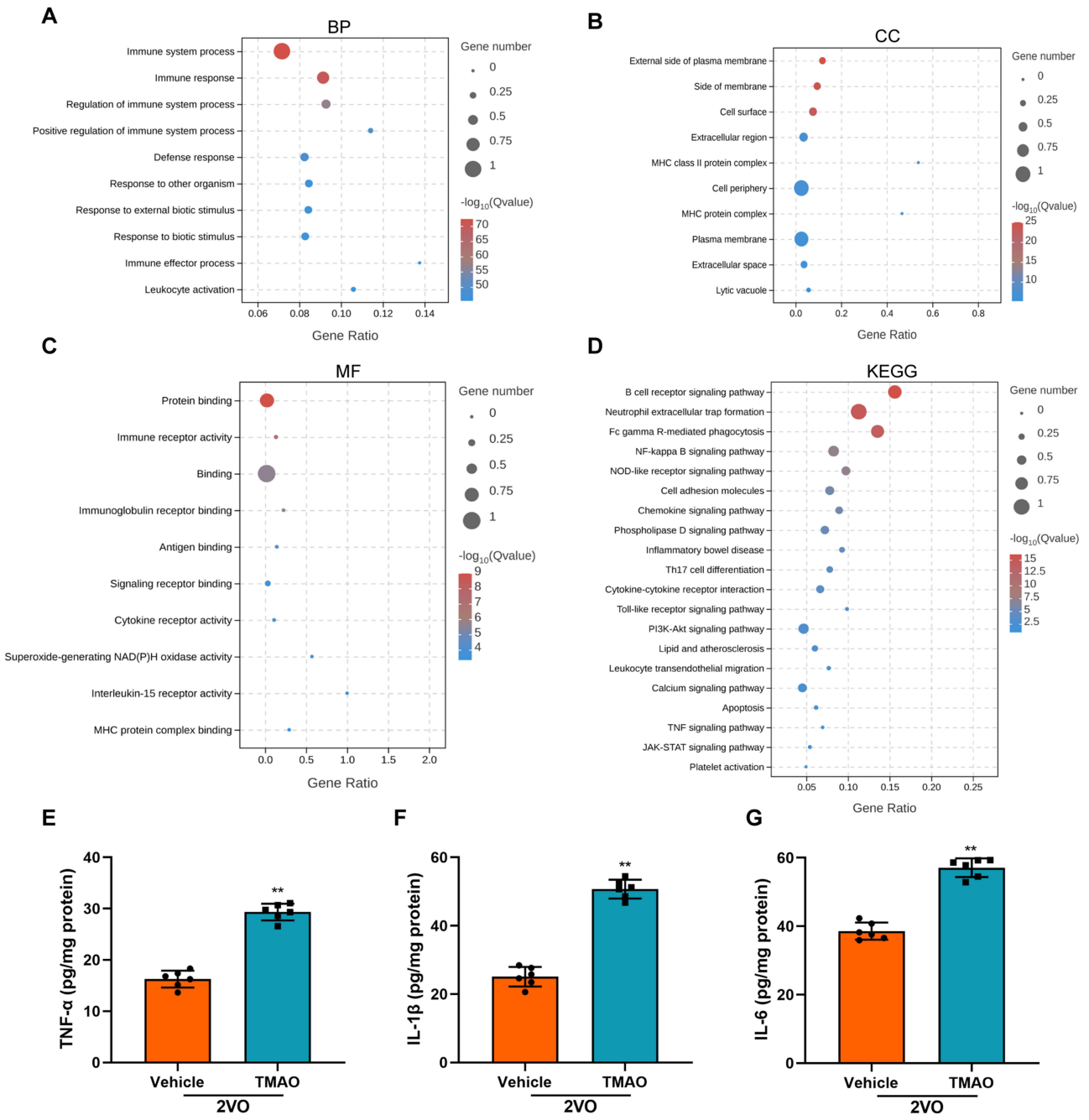

Figure 2 TMAO promoted hippocampal inflammatory response within 2VO Rats. GO enrichment analysis was performed using. (**A**) biological process (BP), (**B**) cellular component (CC) and (**C**) molecular function (MF). The x-axis indicates the number of genes enriched and the y-axis indicates the GO terms. The color represents significance. (**D**) KEGG enrichment analysis was performed. The inflammation-related indexes (**E**) TNF-α, (**F**) IL-1β, (**G**) IL-6 in the hippocampus of 2VO rats were detected by ELISA (n = 6). Datasets reflect the mean ± SD. ** $P < 0.01$ versus the 2VO+Vehicle group.

(PCA) was performed on the expression levels of lncRNAs to investigate the relationship between the two groups (2VO and 2VO+TMAO) samples. It can be found that the DEGs clusters of the samples in 2VO and 2VO+TMAO groups were separated (Figure 3A), indicating that different treatments have a significant effect on transcriptome profiles. The volcano plot revealed that a total of 56 differentially expressed lncRNAs were identified, of which 19 lncRNAs upregulated and 37 lncRNAs down-regulated (Figure 3B). The heat map showed the DEGs of the top 15 up-regulated and down-regulated lncRNAs (Figure 3C). According to previous reports, Fendrr could activate intracerebral inflammation in mice with diabetic cerebral I/R injury.[19] Furthermore, the knockdown of Fendrr reduced pro-inflammatory cytokine secretion in

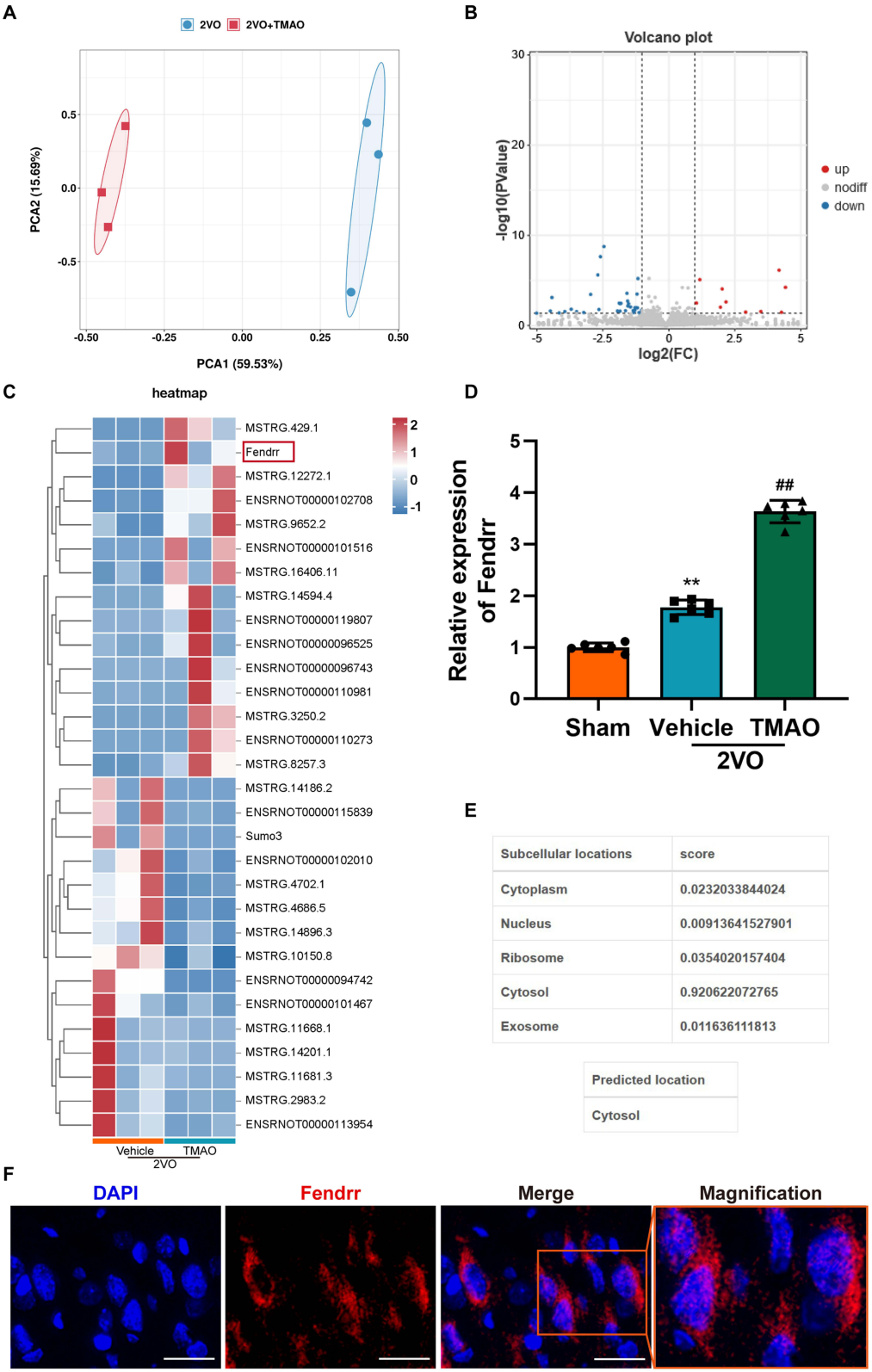

Subcellular locations	score
Cytoplasm	0.0232033844024
Nucleus	0.00913641527901
Ribosome	0.0354020157404
Cytosol	0.920622072765
Exosome	0.011636111813

Predicted location
Cytosol

Figure 3 TMAO up-regulates hippocampal lncRNA Fendrr expression in 2VO Rats. (**A**) PCA of lncRNAs in hippocampal tissues of 2VO and TMAO-treated 2VO rats. (**B**) Volcano plots shows the lncRNA sequencing results of up- and downregulated lncRNAs in hippocampal tissues from 2VO rats treated with TMAO compared with the 2VO rats. (**C**) The heat map shows the DEGs of the top 15 up-regulated and down-regulated lncRNAs. Red represents genetic upregulation, while blue represents genetic downregulation. (**D**) The expression of Fendrr in hippocampus of rats was tested by RT-qPCR (n = 6). (**E**) The subcellular localization of Fendrr was predicted by lncLocator software. (**F**) The subcellular localization of Fendrr was validated by FISH in cells of hippocampus of 2VO rats. Scale bar, 20 μm; Blue: DAPI; red: Fendrr. Datasets reflect the mean ± SD. ** $P < 0.01$ versus the Sham group. ## $P < 0.01$ versus the 2VO+Vehicle group.

caerulein or lipopolysaccharide-induced acute pancreatitis (AP) mouse model.[34] Hence, we hypothesized that the detrimental effect of TMAO on VaD was dependent on Fendrr. At first, Fendrr expression was measured by RT-qPCR in the hippocampal tissues of 2VO and TMAO-treated 2VO rats, and the expression of Fendrr was found to be obviously elevated in the 2VO group, which was more pronounced in the TMAO-treated 2VO rats (Figure 3D). Next, we predicted and validated the subcellular localization of Fendrr. The lncLocator software result indicated that Fendrr was localized in both the nucleus and the cytoplasm and was mainly located in the cytoplasm (Figure 3E). As predicted, FISH experiments further confirmed that Fendrr was located in the cytoplasm (Figure 3F).

Knockdown of Fendrr Can Significantly Improve Neurological Function Injury in 2VO Rats

To investigate the effects of Fendrr on neurological function in 2VO rats, lentivirus vectors knocking down Fendrr (LV-sh -Fendrr) and the negative control LV-sh-NC were injected stereotactically into the bilateral hippocampus of rats and the the knockout efficiency of Fendrr was measured. RT-qPCR result indicated that Fendrr expression was significantly reduced following sh-Fendrr intervention (Figure 4A). Next, OFT and MWM assays were performed to evaluate the spatial learning and memory capacity of the rats, and our findings revealed that the total distance traveled and the percentage of time spent in the center were substantially higher in the sh-Fendrr group when compared to the sh-NC group (Figure 4B–D). Later, MWM dataset suggested that the mean escape latency was decreased when Fendrr was knocked down (Figure 4E). A notable difference in swimming speed did not exist between the two groups (Figure 4F). These observations together demonstrated that knockdown of Fendrr could significantly improve the cognitive function deficits of 2VO rats. Furthermore, Nissl staining assessed the effect of Fendrr knockdown on hippocampal neuronal damage in 2VO rats. Injected with sh-Fendrr considerably increased the Nissl-positive cells in the CA1 region of hippocampus in comparison with the rats injected with sh-NC (Figure 4G and H). Afterward, we tested the inflammatory parameters levels in rat hippocampus by ELISA and found that in 2VO rats injected with sh-Fendrr, TNF-α, IL-1β and IL-6 were suppressed in comparison with vector group (Figure 4I–K). In summary, these data indicated that down-regulation of Fendrr inhibited the inflammatory response in hippocampal tissue and attenuated cognitive impairment in 2VO rats.

Fendrr Negatively Regulates miR-145-5p Expression

There is increasing evidence that lncRNAs can be competing endogenous RNAs (ceRNAs) to bind miRNAs by sequence complementarity, which in turn is involved in the regulation the occurrence and development of disease.[35–37] The experiments described above have shown that Fendrr is mainly localized in the cytoplasm, so we speculated that Fendrr can sponge miRNAs via ceRNA. As shown in Figure 5A, through miRDB database prediction, it was found that there are 14 miRNAs that may be potential targets of Fendrr. Among them, only miR-145-5p was studied and reported to find its expression decreased in the cortex of 2VO rats.[23] Besides, some studies have reported that miR-145-5p had a negative correlation with inflammation. For instance, miR-145-5p could attenuate the apoptosis, oxidative stress and inflammatory response through the inhibition of NOH-1, eventually reducing myocardial I/R damage.[24] The exosomes containing miR-145-5p could attenuate inflammatory responses via regulating the TLR4/NF-κB signaling pathway in spinal cord injury.[38] Hence, we selected miR-145-5p as the downstream research target of Fendrr. RNAhybrid (https://bibiserv.cebitec.uni-bielefeld.de/rnahybrid/) was used to predict, and the results implied the potential binding sites between miR-145-5p and Fendrr. The minimum free energy was found < −25kcal/mol (Figure 5B). In addition, the binding sites in the Starbase database (http://starbase.sysu.edu.cn) were consistent with the predicted results (Figure 5C). Afterward, the binding relationship was further validated by dual luciferase reporter assays and RIP assays. The luciferase activity of Fendrr-WT was greatly reduced with transfection of agomir-145-5p in the dual luciferase reporter, whereas Fendrr-MUT showed no significant difference (Figure 5D). RIP experiments demonstrated enhanced enrichment of Fendrr and miR-145-5p under Ago2 treatment under Ago2 treatment (Figure 5E). Moreover, we detected their co-localization in hippocampal tissue by FISH, and discovered that Fendrr and miR-145-5p co-localized in the cytoplasm of hippocampal tissue (Figure 5F).

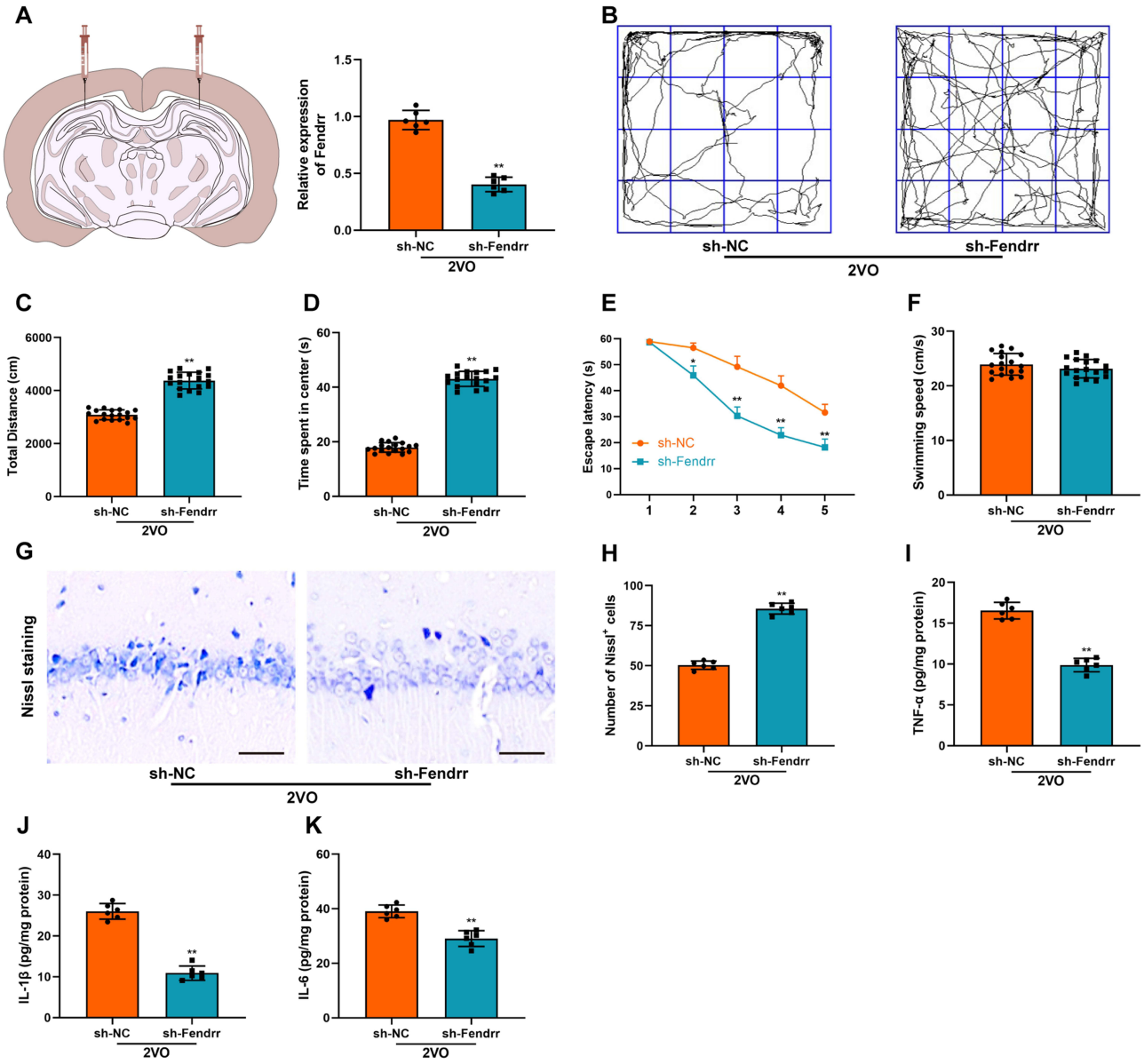

Figure 4 Knockdown of Fendrr can significantly improve neurological function injury in 2VO rats. (**A**) The schematic diagram of lentiviral vectors injected stereotactically into the bilateral hippocampus of rats and the efficiency of knockdown of Fendrr expression was tested by RT-qPCR (n = 6). (**B**) Representational movement tracks, (**C**) total distance traveled and (**D**) time spent in the center in each group were measured using the OFT (n = 18). (**E**) The escape latency and (**F**) swimming speeds in each group were recorded by MWM (n = 18). (**G**) Neuronal damage in the CA1 region of the hippocampus was assessed by Nissl staining in each group of rats. Scale bar, 20 μm (n = 6). (**H**) The bar chart shows the quantification of the Nissl-positive cells (n = 6). The inflammation-related indexes (**I**) TNF-α, (**J**) IL-1β, (**K**) IL-6 in the hippocampus of 2VO rats were detected by ELISA (n = 6). Datasets reflect the mean ± SD. * $P < 0.05$ and ** $P < 0.01$ versus the 2VO+sh-NC group.

Furthermore, we examined the expression of miR-145-5p in 2VO rats injected with sh-Fendrr and detected upregulation of miR-145-5p (Figure 5G). Shortly, miR-145-5p is a target gene of Fendrr and can be negatively regulated by Fendrr.

Upregulation of miR-145-5p Can Reduce Neurological Function Injury in 2VO Rats

Based on the above studies, we first detected miR-145-5p expression in hippocampus of rats in sham-operated and 2VO groups, and the outcomes showed that miR-145-5p did display low levels in 2VO rats (Figure 6A). We implemented miR-145-5p up-regulation assay in rats and the RT-qPCR outcome indicated that the expression of miR-145-5p was amplified by the injection with agomir-145-5p (Figure 6B). In behavioral tests, we observed that the total distance traveled and the percentage of time spent in the center was significantly increased in agomir-145-5p group (Figure 6C–

A

Target Detail	Target Rank	Target Score	miRNA Name	Gene Symbol
Details	1	81	rno-miR-743b-5p	submission
Details	2	71	rno-miR-298-5p	submission
Details	3	71	rno-miR-155-5p	submission
Details	4	60	rno-miR-191a-3p	submission
Details	5	60	rno-miR-17-2-3p	submission
Details	6	58	rno-miR-145-5p	submission
Details	7	55	rno-miR-126b	submission
Details	8	53	rno-miR-133c	submission
Details	9	52	rno-miR-18a-3p	submission
Details	10	52	rno-miR-873-5p	submission
Details	11	52	rno-miR-20b-3p	submission
Details	12	52	rno-miR-17-1-3p	submission
Details	13	50	rno-miR-3552	submission
Details	14	50	rno-miR-126a-5p	submission

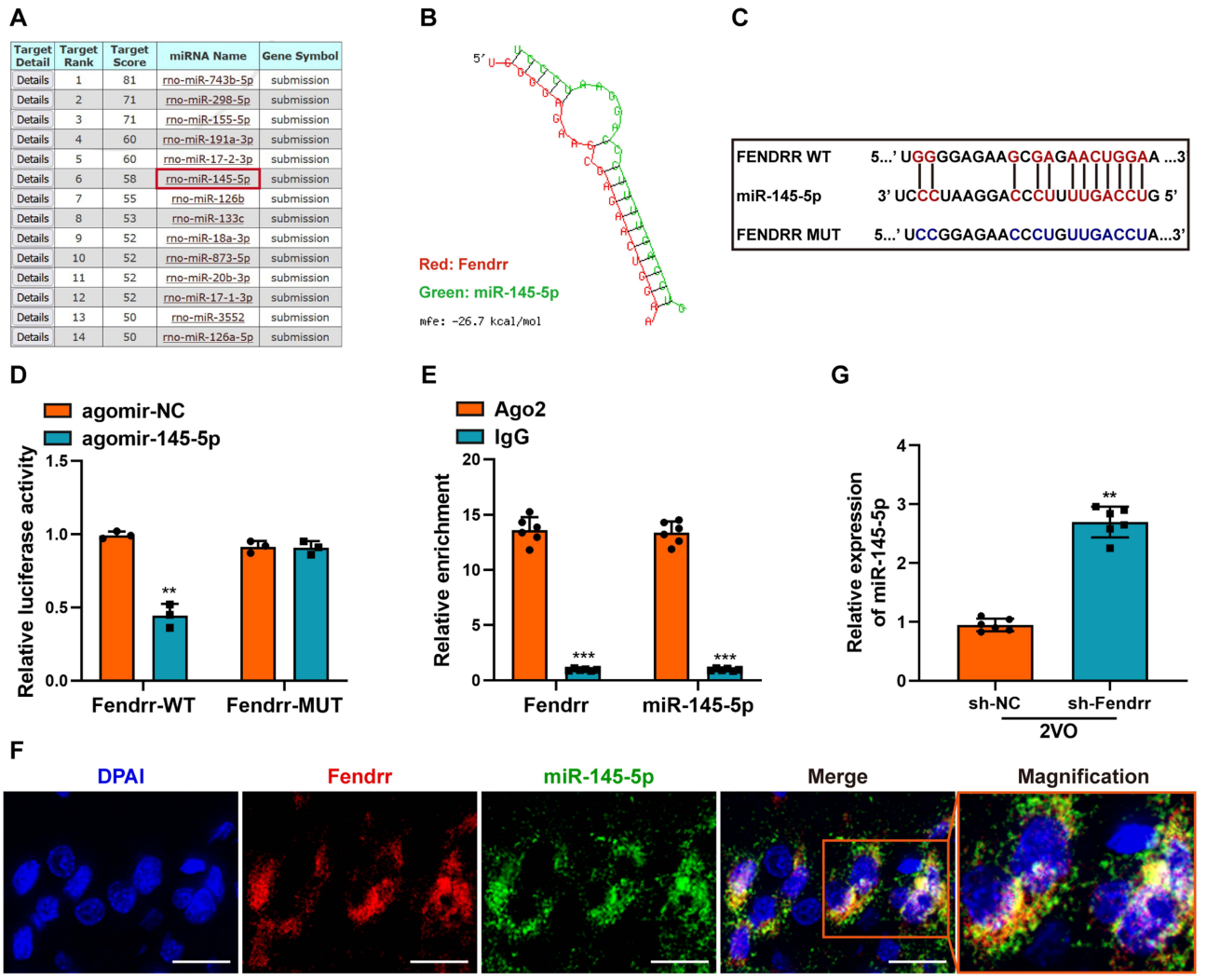

Figure 5 Fendrr negatively regulates miR-145-5p expression. (**A**) The 14 potential targets of Fendrr were predicted by miRDB database. (**B**) The binding sites between miR-145-5p and Fendrr and the minimum free energy were predicted by RNAhybrid. (**C**) The binding sites between Fendrr and miR-145-5p were predicted by Starbase database. (**D**) The binding relation between Fendrr and miR-145-5p was validated through dual luciferase reporter assays (n = 3). (**E**) The enrichment level of Fendrr and miR-145-5p was detected by RIP assay (n = 6). (**F**) The Fendrr and miR-145-5p co-localization in hippocampal tissue was detected by FISH. Scale bar, 20 μm; Blue: DAPI; red: Fendrr; green: miR-145-5p. (**G**) The miR-145-5p expression was examined by RT-qPCR after the down-regulation of Fendrr (n = 6). Datasets reflect the mean ± SD. ** $P < 0.01$ versus the agomir-NC group or 2VO+sh-NC group; *** $P < 0.001$ versus the Ago2 group.

E), while the mean escape latency was significantly lowered (Figure 6F). Significant differences in swimming speed did not exist between the two groups (Figure 6G). Histological observation of brain tissues depicted an increase in the number of Nissl bodies in the CA1 region of rat hippocampal after treatment of agomir-145-5p (Figure 6H and I). Besides, ELISA assay results uncovered obvious decreases in TNF-α, IL-1β, and IL-6 concentrations in 2VO rats with overexpression of miR-145-5p (Figure 6J–L). Therefore, the amplification of miR-145-5p was found to improve neurological function recovery in 2VO rats.

PXN is the Target of miR-145-5p

In order to have a further investigation of the possible targets of miR-145-5p, we used three bioinformatics tools, TargetScan, miRDB and miRMap to predict the targets of miR-145-5p. There were a sum of 122 genes located in cross-sets of three databases (Figure 7A). In addition, we plotted the corresponding lncRNA-miRNA-mRNAs interaction network on the basis of predicted results (Figure 7B). Among these candidate genes, Trim2, PXN, and Nedd4l were reported to be significantly upregulated in the cortex of 2VO rats.[23,39] Then, the minimum free energies of binding

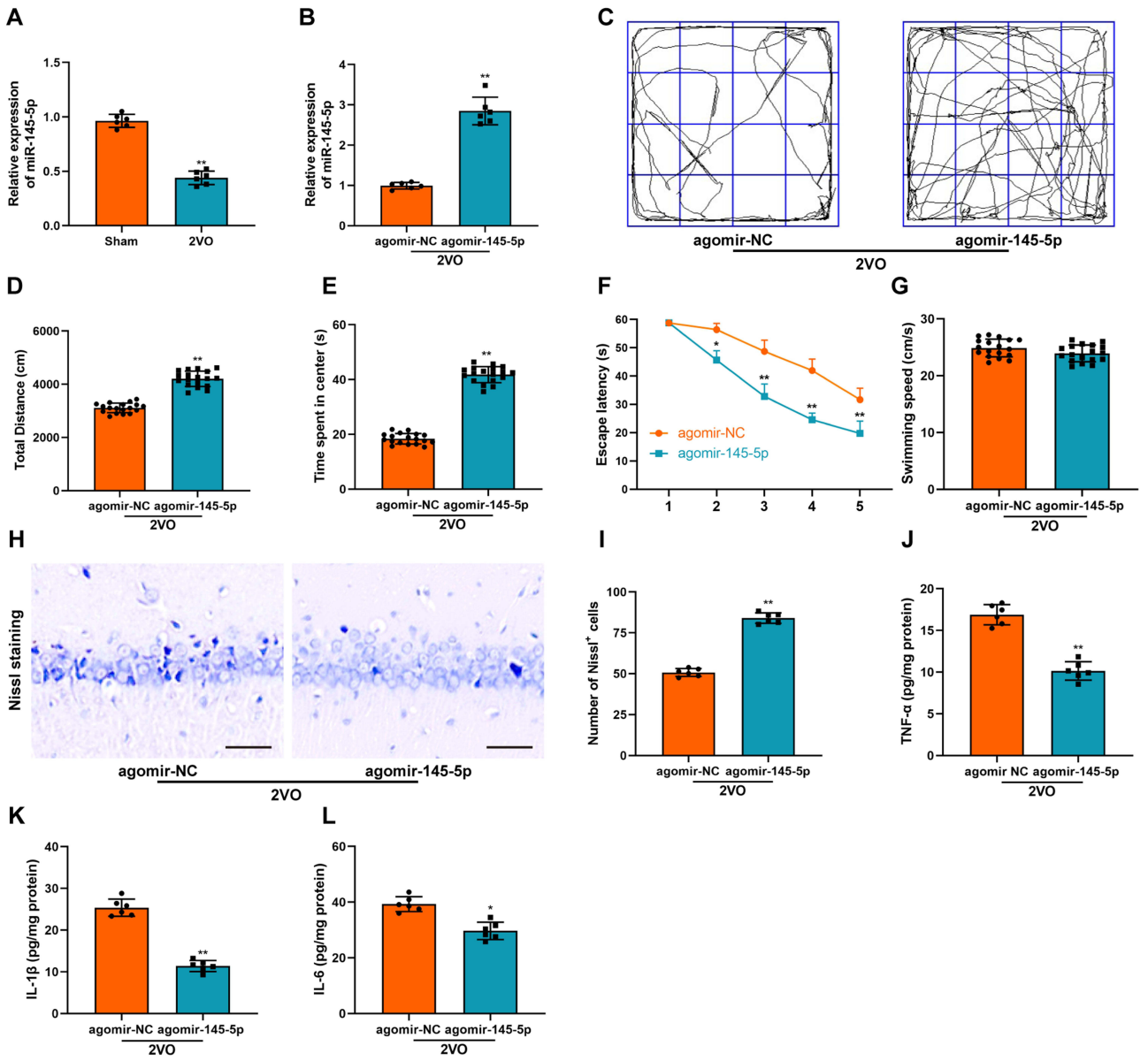

Figure 6 Upregulation of miR-145-5p can reduce neurological function injury in 2VO rats. (**A**) The expression of miR-145-5p in hippocampus of rats was tested by RT-qPCR (n = 6). (**B**) The efficiency of upregulation of miR-145-5p expression was tested by RT-qPCR (n = 6). (**C**) Representational movement tracks, (**D**) total distance traveled and (**E**) time spent in the center in each group were measured using the OFT (n = 18). (**F**) The escape latency and (**G**) swimming speeds in each group were recorded by MWM (n = 18). (**H**) Neuronal damage in the CA1 region of the hippocampus was assessed by Nissl staining in each group of rats. Scale bar, 20 μm (n = 6). (**I**) The bar chart shows the quantification of the Nissl-positive cells (n = 6). The inflammation-related indexes (**J**) TNF-α, (**K**) IL-1β, (**L**) IL-6 in the hippocampus of 2VO rats were detected by ELISA. Datasets reflect the mean ± SD. * $P < 0.05$ versus the 2VO+agomir-NC group; ** $P < 0.01$ versus the Sham group or 2VO+agomir-NC group.

between them and miR-145-5p were −31.5, −35.1, and −32.8 kcal/mol, respectively, predicted by the RNAhybrid (Figure 7C), which suggested that PXN is most likely to bind to miR-145-5p. Also, Targetscan database predictions indicated that a potential binding region existed between miR-145-5p and PXN (Figure 7D). Similarly, dual luciferase reporter gene assays further clarified the binding of miR-145-5p to PXN. The luciferase activity was clearly decreased in cells transfected with agomir-145-5p and WT-PXN (Figure 7E). RIP experiment displayed the augmented enrichment of miR-145-5p and PXN under Ago2 treatment (Figure 7F). In addition, FISH analysis revealed that miR-145-5p and PXN co-localize in the cytoplasm of the hippocampus tissues (Figure 7G). Next, we detected the miR-145-5p effect on PXN level, and found that the expression of PXN was inhibited after miR-145-5p up-regulation in RT-qPCR and Western Blot assay (Figure 7H–J). The above results demonstrated that PXN is a downstream target of miR-145-5p.

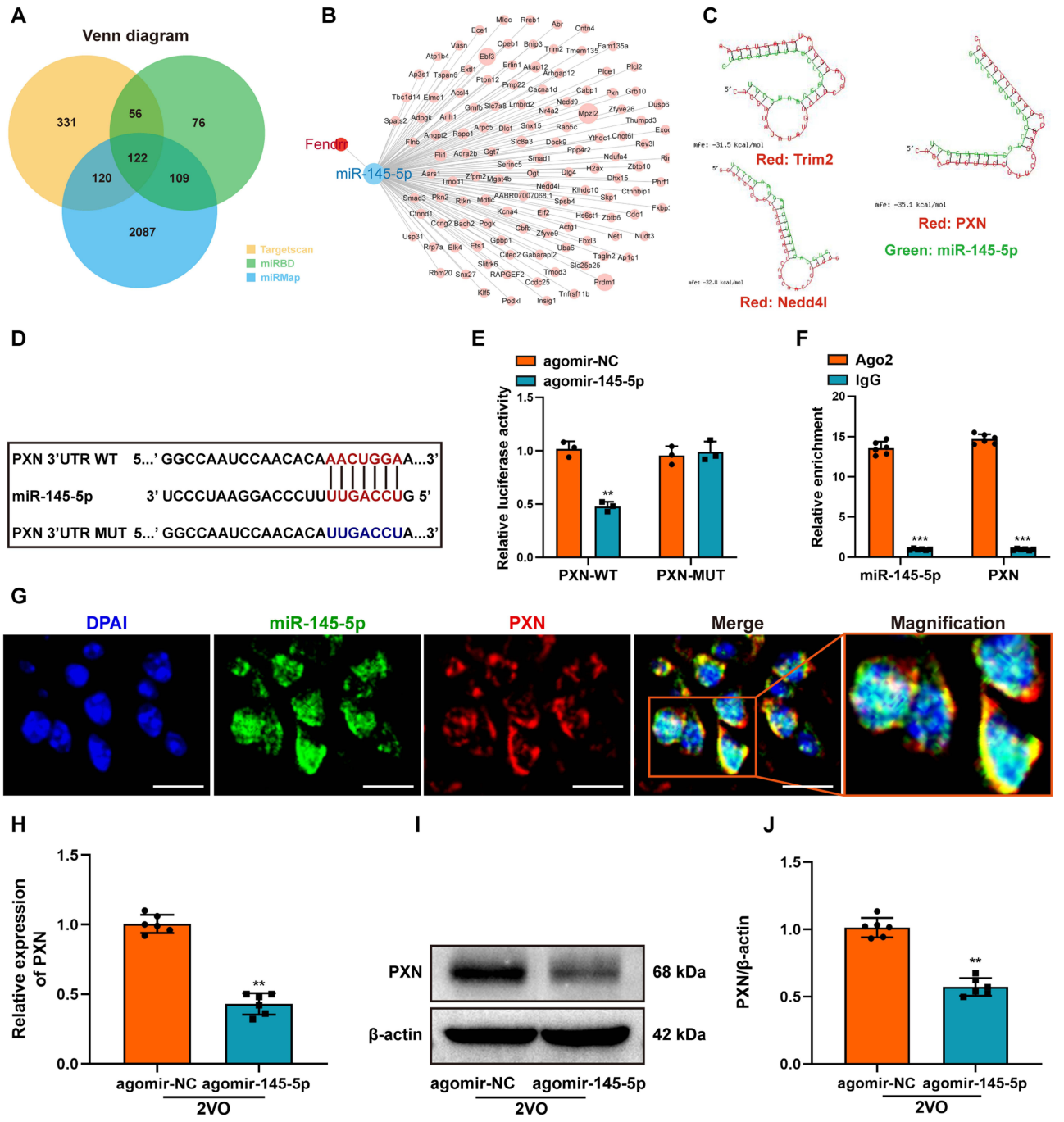

Figure 7 miR-145-5p targets PXN. (**A**) The potential targets of miR-145-5p were predicted by three bioinformatics analysis tools. (**B**) The lncRNA-miRNA-mRNAs interaction network on the basis of predicted results. (**C**) The binding sites between candidate genes and miR-145-5p and the minimum free energy were predicted by RNAhybrid. (**D**) The binding sites between miR-145-5p and PXN were predicted by Targetscan database. (**E**) The binding relation between miR-145-5p and PXN was validated through dual luciferase reporter assays (n = 3). (**F**) The enrichment level of Fendrr and miR-145-5p was detected by RIP assay (n = 6). (**G**) The miR-145-5p and PXN co-localization in hippocampal tissue was detected by FISH. Scale bar, 20 μm; Blue: DAPI; red: PXN; green: miR-145-5p. (**H**) The PXN expression was examined by RT-qPCR after the up-regulation of miR-145-5p (n = 6). (**I**) The PXN expression was detected by Western Blot after the up-regulation of miR-145-5p. (**J**) The bar chart shows quantification for PXN expression (n = 6). Datasets reflect the mean ± SD. ** $P < 0.01$ versus the agomir-NC group or 2VO+agomir-NC group; *** $P < 0.001$ versus the Ago2 group.

Knockdown of PXN Can Reduce Neurological Function Injury in 2VO Rats

To explore the effect of PXN on VaD, we first found that PXN expression in the hippocampus of 2VO rats were increased by RT-qPCR and Western Blot (Figure 8A–C). Then LV-sh-NC and LV-sh-PXN were injected into the bilateral

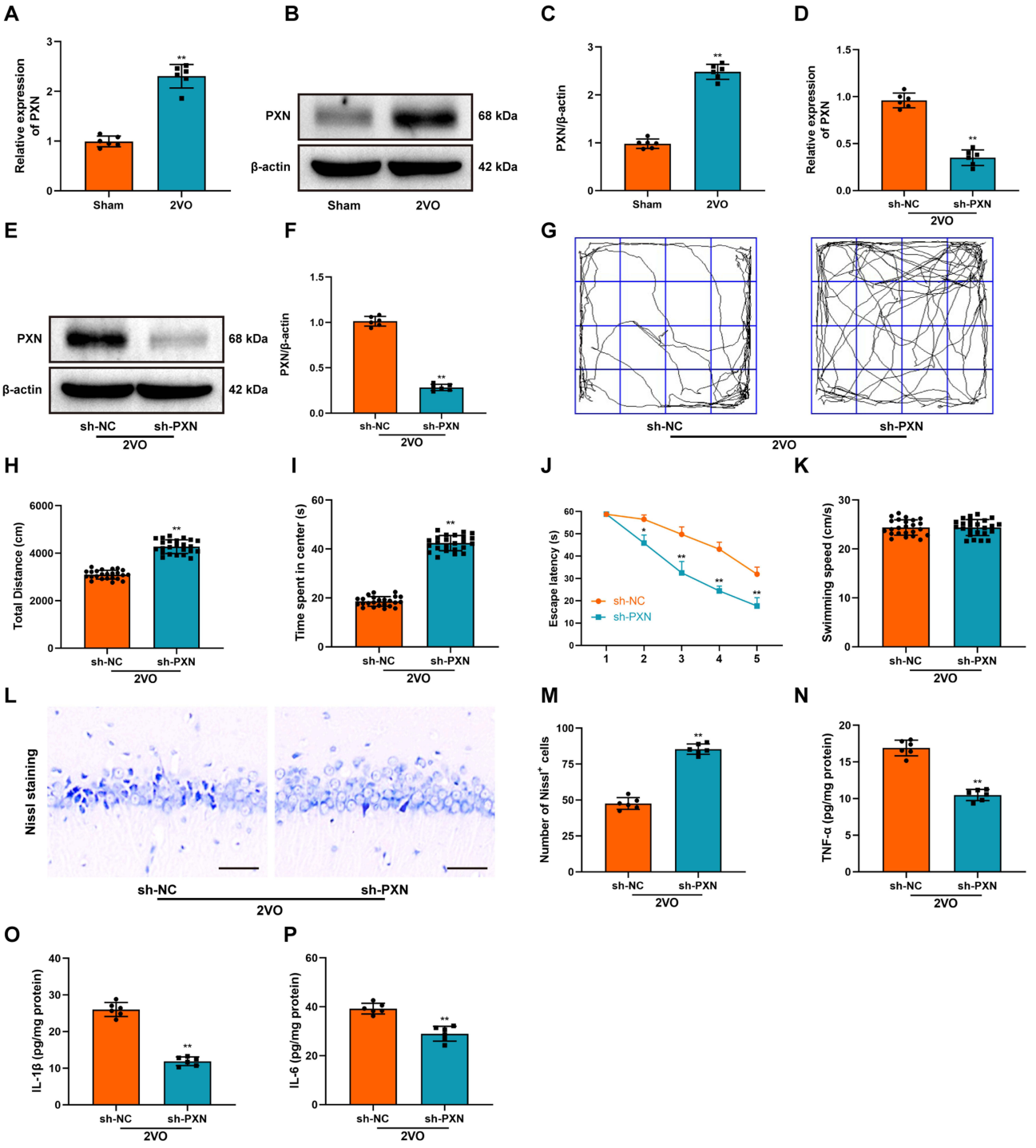

Figure 8 Knockdown of PXN can reduce neurological function injury in 2VO rats. (**A**) The expression of PXN in hippocampus of rats was detected by RT-qPCR (n = 6). (**B**) The expression of PXN in hippocampus of rats was tested by Western Blot. (**C**) The bar chart shows quantification for PXN expression (n = 6). (**D**) The knockdown efficiency of PXN expression was detected by RT-qPCR (n = 6). (**E**) The efficiency of knockdown of PXN expression was detected by Western Blot. (**F**) The bar chart shows quantification for PXN expression (n = 6). (**G**) Representational movement tracks, (**H**) total distance traveled and (**I**) time spent in the center in each group were measured using the OFT (n = 24). (**J**) The escape latency and (**K**) swimming speeds in each group were recorded by MWM (n = 24). (**L**) Neuronal damage in the CA1 region of the hippocampus was assessed by Nissl staining in each group of rats. Scale bar, 20 μm (n = 6). (**M**) The bar chart shows the quantification of the Nissl-positive cells (n = 6). The inflammation-related indexes (**N**) TNF-α, (**O**) IL-1β, (**P**) IL-6 in the hippocampus of 2VO rats were detected by ELISA (n = 6). Datasets reflect the mean ± SD. * $P < 0.05$ versus the 2VO+sh-NC group; ** $P < 0.01$ versus the Sham group or 2VO+sh-NC group.

hippocampus of 2VO model rats, respectively. RT-qPCR and Western Blot confirmed that injection of sh-PXN significantly lowered the expression of PXN in 2VO rats (Figure 8D–F). After silencing PXN, it was found that the

learning and spatial memory abilities of rats were significantly reduced (Figure 8G–J). The specific performances were an increase in the percentage of time spent in the center and the total distance traveled, and a decrease of the mean escape latency. A notable difference in swimming speed did not exist between the two groups (Figure 8K). Moreover, in 2VO rats injected with sh-PXN, there were increased Nissl bodies in the hippocampal CA1 region (Figure 8L and M). The inflammatory parameters were also explored in the hippocampus, with the results presenting that concentrations of TNF-α, IL-1β and IL-6 were suppressed (Figure 8N–P). Overall, down-regulating PXN promoted the recovery of neurologic function in 2VO rats.

Inhibition of miR-145-5p Reversed the Fendrr Knockdown-Mediated Influence on 2VO Rats

In the hippocampus of 2VO rats, we noticed that PXN expression went down-regulate after treatment of sh-Fendrr (Figure 9A–C). In this regard, to verify whether Fendrr affects VaD through miR-145-5p/PXN axis, rats were stereotactically injected with sh-Fendrr and antagomir-145-5p and the negative control lentivirus vectors into the bilateral hippocampus, respectively. In 2VO rats, injection of sh-Fendrr would enhance neurological function, including the improvement of behavioral tests and the increase in the number of Nissl bodies in the CA1 region of the hippocampus, while the effects of sh-Fendrr would be weakened by antagomir-145-5p (Figure 9D–J). In addition, the silenced miR-145-5p reversed the decrease in PXN expression by sh-Fendrr (Figure 9K–M) and suppression of inflammatory response (Figure 9N–P). In summary, Fendrr exacerbated neurological impairment and inflammatory responses in 2VO rats by targeting PXN via sponge miR-145-5p.

TMAO Aggravated the Neurological Function of 2VO Rats by Upregulating Fendrr Targeting miR-145-5p

To investigate whether TMAO exacerbates VaD injury by regulating Fendrr/miR-145-5p expression, we stereotactically injected the sh-Fendrr and antagomir-145-5p into the bilateral hippocampus of TMAO-administrated 2VO rats. After sh-Fendrr injection, the 2VO rats administered with TMAO have the increased percentage of time spent in the center and total distance traveled, while the decreased mean escape latency. But, these effects of sh-Fendrr were reversed via the inhibition of miR-145-5p (Figure 10A–D). Notable differences in swimming speed did not exist among groups (Figure 10E). Nissl staining elicited that sh-Fendrr ameliorated hippocampal tissue damage in TMAO-treated 2VO rats, but the inhibition of miR-145-5p expression remarkably abolished this effect (Figure 10F and G). Besides, injection of sh-Fendrr attenuated the upregulation of PXN in TMAO-treated 2VO rats, but injection of antagomir-145-5p reversed this expression (Figure 10H–J). The decrease in miR-145-5p counteracted the suppressive effects of Fendrr on the inflammatory cytokines in TMAO-treated 2VO rats (Figure 10K–M). Collectively, TMAO impaired neural function in 2VO rats by affecting the expression of Fendrr/miR-145-5p.

Discussion

VaD, featuring degradation of memory and cognitive capacity, is the second most common form of dementia due to chronic cerebral underperfusion.[40] In our previous investigation, we demonstrated that increased circulating TMAO could exacerbate cognitive impairment in VaD rats.[14] However, the molecular mechanism of the TMAO-promoted VaD injury remains unknown. The current research is the first to confirm that upregulation of Fendrr induced by TMAO is implicated in the pathogenesis of VaD. TMAO aggravated neuro-inflammation and cognitive dysfunction via Fendrr/miR-145-5p/PXN axis in VaD rats (Figure 11).

Several new evidence emphasizes that pathological changes in VaD lead to excessive neuroinflammation, which further causes various forms of cell death including neurons.[41–43] There are two ways to induce VaD in experimental animals: temporary occlusion of the middle cerebral artery or permanent occlusion of the common carotid artery.[44] Of these, the 2VO rat model is one of the most widely used animal models of VaD,[45] which can reproduce the CCH situation and cognitive impairment observed in VaD patients. Notably, a previous study conducted the GO and KEGG enrichment analysis of differentially expressed miRNA/TF-associated genes in the cortex of 2VO rats and found that these genes

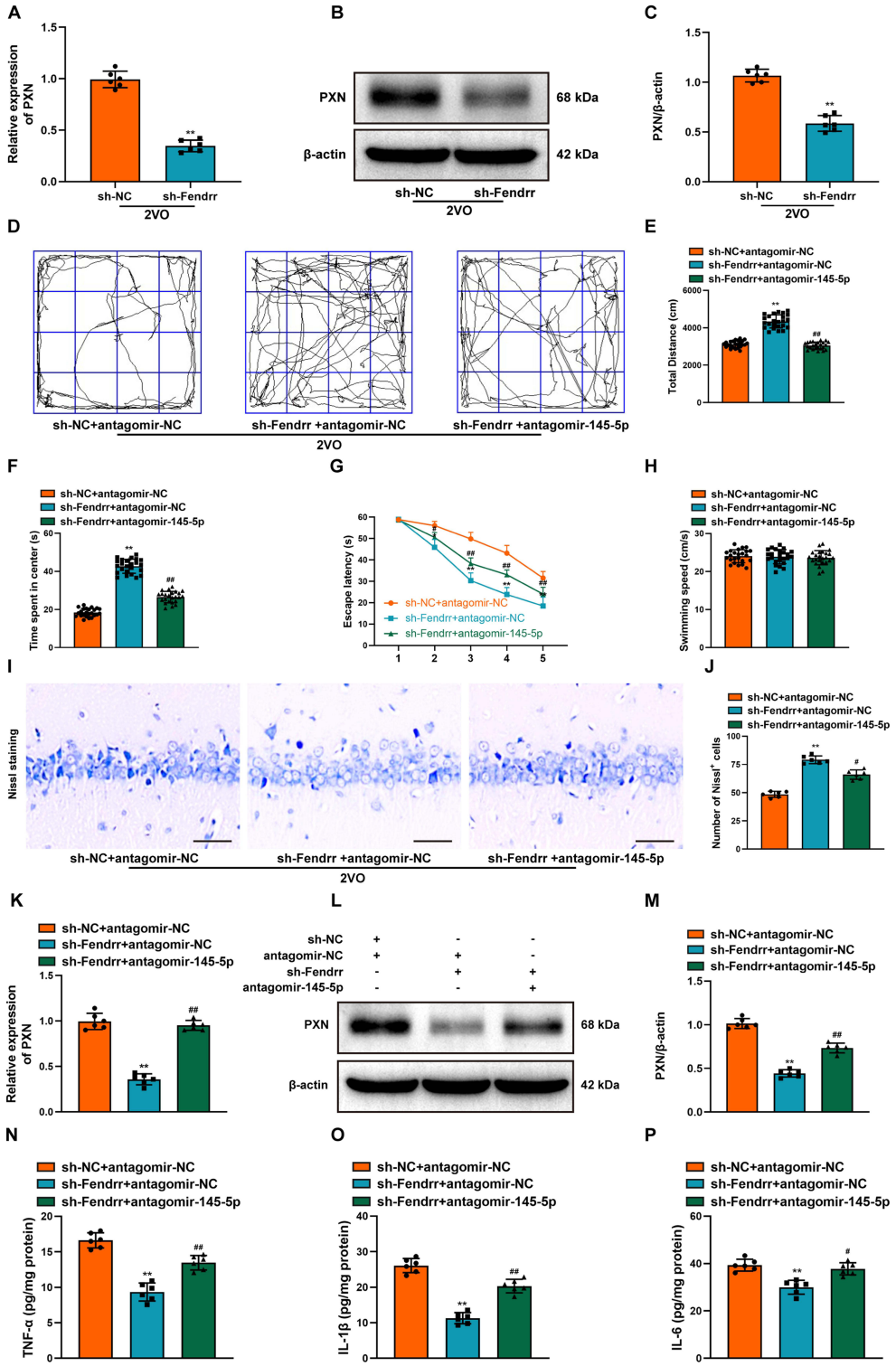

Figure 9 Inhibition of miR-145-5p reversed the Fendrr knockdown-mediated influence on 2VO rats. (**A**) The PXN expression was examined by RT-qPCR after the down-regulation of Fendrr (n = 6). (**B**) The PXN expression was examined by Western Blot after the down-regulation of Fendrr. (**C**) The bar chart shows quantification for PXN expression (n = 6). (**D**) Representational movement tracks, (**E**) total distance traveled and (**F**) time spent in the center in each group were measured using the OFT (n = 24). (**G**) The escape latency and (**H**) swimming speeds in each group were recorded by MWM (n = 24). (**I**) Neuronal damage in the CA1 region of the hippocampus was assessed by Nissl staining in each group of rats. Scale bar, 20 μm (n = 6). (**J**) The bar chart shows the quantification of the Nissl-positive cells (n = 6). (**K**) The PXN expression was examined by RT-qPCR after the down-regulation of Fendrr and down-regulation of miR-145-5p (n = 6). (**L**) The PXN expression was examined by Western Blot after the down-regulation of Fendrr and down-regulation of miR-145-5p (n = 6). (**M**) The bar chart shows quantification for PXN expression (n = 6). The inflammation-related indexes (**N**) TNF-α, (**O**) IL-1β, (**P**) IL-6 in the hippocampus of 2VO rats were detected by ELISA (n = 6). Datasets reflect the mean ± SD. * $P < 0.05$ versus the 2VO+sh-NC+antagomir-NC group; ** $P < 0.01$ versus the 2VO+sh-NC group or 2VO+sh-NC+antagomir-NC group; $^{\#}P < 0.05$ and $^{\#\#}P < 0.01$ versus the 2VO+sh-Fendrr+antagomir-NC group.

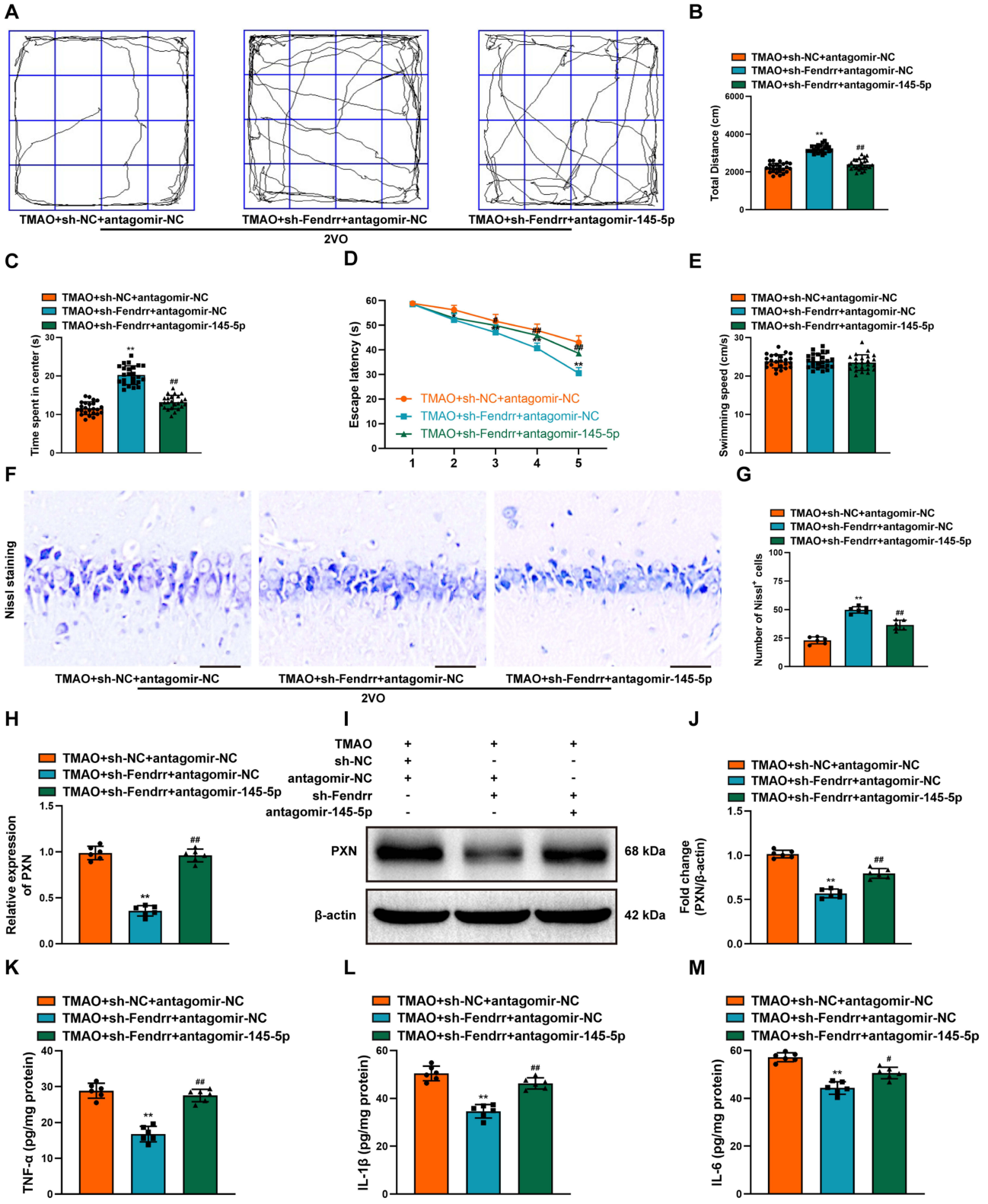

Figure 10 TMAO aggravated the neurological function of 2VO rats by upregulating Fendrr targeting miR-145-5p. (**A**) Representational movement tracks, (**B**) total distance traveled and (**C**) time spent in the center in each group were measured using the OFT (n = 24). (**D**) The escape latency and (**E**) swimming speeds in each group were recorded by MWM (n = 24). (**F**) Neuronal damage in the CA1 region of the hippocampus was assessed by Nissl staining in each group of rats. Scale bar, 20 μm (n = 6). (**G**) The bar chart shows the quantification of the Nissl-positive cells (n = 6). (**H**) The PXN expression was detected by RT-qPCR after the down-regulation of Fendrr and down-regulation of miR-145-5p in TMAO-treated 2VO rats (n = 6). (**I**) The PXN expression was detected by Western Blot after the down-regulation of Fendrr and down-regulation of miR-145-5p in TMAO-treated 2VO rats (n = 6). (**J**) The bar chart shows quantification for PXN expression (n = 6). The inflammation-related indexes (**K**) TNF-α, (**L**) IL-1β, (**M**) IL-6 in the hippocampus of TMAO-treated 2VO were detected by ELISA (n = 6). Datasets reflect the mean ± SD. * $P < 0.05$ and ** $P < 0.01$ versus the TMAO+sh-NC+antagomir-NC group; # $P < 0.05$ and ## $P < 0.01$ versus the TMAO+sh-Fendrr+antagomir-NC group.

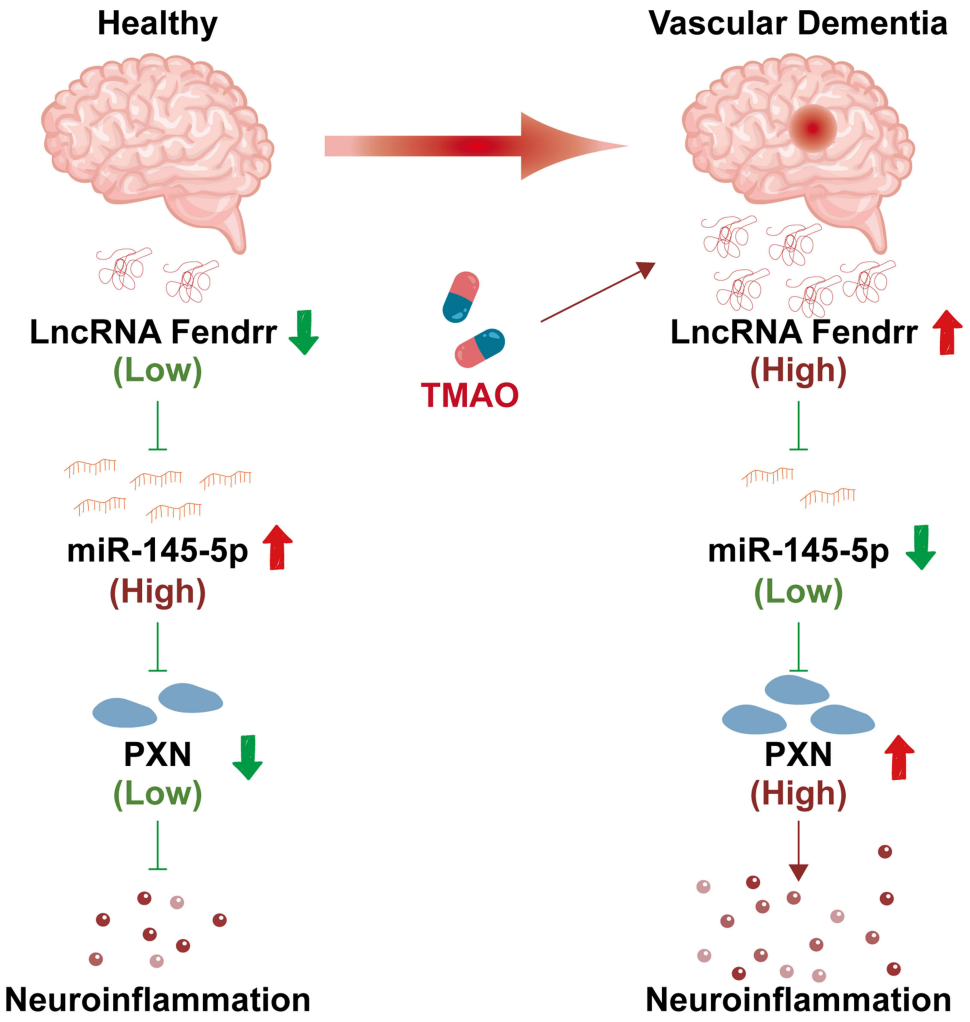

Figure 11 The mechanism of action of TMAO on neuroinflammation after VaD. TMAO can promote neuroinflammation and aggravate neural damage in vascular dementia by regulating the lncRNA Fendrr/miR-145-5p/PXN axis.

were primarily connected to hypoxia, inflammation and apoptosis pathways of VaD.[23] Similarly, we performed KEGG analysis of DEGs in the hippocampus of TMAO-treated 2VO rats and found that pathways involving target genes were also associated with the regulation of inflammation and cellular immunity. Inflammasomes are important mediators and key switches of inflammation, among which the most representative is the NLRP3 inflammasome. As part of the innate immune system, the NLRP3 inflammasome has been shown to participate in the pathogenesis of CCH-induced VaD by regulating neuroinflammation.[46] NLRP3 binds to ASC as a scaffold, thereby recruiting and activating caspase-1. Activated caspase-1 catalyzes the degradation of pro-interleukin-1β (IL-1β) and pro-interleukin-18 (IL-18) into biologically active mature forms,[47] ultimately leading to an inflammatory response and upregulating the gene expression of several inflammatory mediators.[48] Besides, our previous study has already uncovered that the protein expression of NLRP3 and IL-1β in the hippocampus of 2VO rats was significantly upregulated, and further increased after TMAO treatment.[14] Accordingly, we examined the changes in inflammatory mediators TNF-α, IL-1β, and IL-6 in the hippocampus of 2VO rats. The results suggested that the levels of TNF-α, IL-1β, and IL-6 in the hippocampus of rats in the 2VO group were markedly elevated, and their expression was further augmented after TMAO administration. This is consistent with the findings of others. Zhang et al have manifested that the high levels of circulating TMAO enhanced the release of inflammatory mediators and increased the NF-kB activity in inflammatory model rats.[49] In addition, elevated circulating TMAO levels downregulated IL-10, exacerbated vascular oxidative stress and inflammation, and resulted in

endothelial dysfunction.[50] Altogether, the above data indicate that TMAO can activate relevant inflammatory pathways and promote the release of neuro-inflammatory mediators in the VaD rat model.

Thereafter, we explored the molecular mechanisms by which TMAO promotes neuroinflammation in VaD. As recorded, TMAO could promote atherosclerosis through regulating the lncRNA enriched abundant transcript 1 (NEAT1).[51] The link between lncRNAs and cognitive impairments has recently gained attention. LncRNA MALAT1 has been observed to target miR-9-3p to upregulate SAP97 in the VaD mice, thereby promoting VaD progression.[52] The knockdown of lncRNA XIST alleviated BACE1 alteration via miR-124/BACE1 signaling pathways in the 2VO-induced Alzheimer's disease model.[53] We analyzed the hippocampus of rats in the 2VO and TMAO-administrated 2VO groups by high-throughput sequencing to screen for differentially expressed lncRNAs. Significantly, the expression of Fendrr in hippocampus of 2VO rats was remarkably elevated after TMAO administration. Fendrr was initially found to be associated with the development of a variety of human malignant tumors, such as prostate cancer, renal cell carcinoma and cervical cancer.[54–56] Of interest, available evidence suggests that Fendrr may regulate pyroptosis and inflammation of microglia in diabetes-cerebral I/R mice.[19] Fendrr could modulate inflammation by binding PRC2 to inhibit the epigenetic role of ATG7 in acute pancreatitis.[34] Nevertheless, the function of Fendrr in VaD is unclear. In this study, we demonstrated that Fendrr expression was significantly increased in the hippocampus of 2VO rats, and TMAO exacerbated this increase in expression. Knockdown of Fendrr inhibited 2VO model-induced deficits in spatial learning and memory, neuronal damage, and elevated inflammatory mediators.

There is growing evidence that lncRNAs could act as sponges for miRNAs and thus mediate gene expression regulation functions.[36,57] Our prediction analysis indicated that Fendrr had binding sites with miR-145-5p. Dual luciferase reporter gene, RIP and FISH assays confirmed the interaction between Fendrr and miR-145-5p. Qi et al discovered that miR-145-5p expression was significantly downregulated in MCAO mice whereas suppressing miR-145-5p enhanced the levels of proinflammatory factors TNF-α and NO in activated microglia cells.[58] Overexpression of miR-145-5p could attenuate inflammatory responses in mouse cardiomyocytes hypoxia/reoxygenation (H/R) modeling.[59] To be noted, a sequencing report found that miR-145-5p is lowly expressed in the cortex of 2VO rats.[23] However, the potential effect of miR-145-5p in VaD has not been identified by the researchers. Similar to previous studies, our data showed that miR-145-5p was downregulated in 2VO-induced VaD model rats. Additionally, restoring miR-145-5p expression suppressed 2VO-induced cognitive impairment, neuronal death and inflammation levels. To our knowledge, we report for the first time the protective effect of miR-145-5p against VaD. To determine whether the effect of Fendrr is dependent on miR-145-5p, we simultaneously injected antagomiR-145-5p and sh-Fendrr into the bilateral hippocampus of 2VO rats, and the results showed that inhibition of miR-145-5p reversed the anti-inflammatory and protective effects of sh-Fendrr on VaD.

Paxillin, as a multi-domain adaptor protein, is expressed in almost all tissues and plays an important role in cell motility, migration, adhesion and growth control.[60] Indeed, miR-145-5p was reported to target PXN to attenuate cardiac hypertrophy caused by angiotensin II.[61] Another literature also stated that miR-145 may act as a colon cancer inhibitor by targeting PXN.[62] Besides, a sequencing result observed that PXN was notably elevated in the cortex of 2VO rats.[23] In this study, we found elevated levels of PXN in the hippocampus of 2VO rats and confirmed that its expression was negatively regulated by miR-145-5p. Moreover, loss-of-function assay of PXN showed that PXN depletion alleviated the neurological impairment in 2VO rats, as evidenced by total distance traveled and the percentage of time spent in the center, and Nissl bodies, and a decrease in mean escape latency. Interestingly, a study by Wang et al pointed out that Paxillin enhanced NLRP3 deubiquitination by recruiting USP13, thereby activating the NLRP3 inflammasome on ATP processing and K^+ efflux.[63] Similarly, it has been claimed that upregulation of PXN may promote inflammation and the development of acute ischemic stroke.[64,65] This hints at an inextricable relationship between PXN and neuroinflammation. Not surprisingly, we discovered that knockdown of PXN was able to reduce the secretion of inflammatory factors TNF-α, IL-1B, and IL-6 by ELSIA assay. Finally, we simultaneously injected sh-Fendrr and antagomiR-145-5p into the bilateral hippocampus of TMAO-treated 2VO rats. The results suggested that the down-expression of Fendrr ameliorated the damaging effects of TMAO on 2VO rats, but suppression of miR-145-5p expression reversed this effect. Thus, these evidences indicated that TMAO exacerbates VaD neural damage by regulating the expression of the Fendrr/miR-145-5p/PXN axis, which provides a potential therapeutic target for VaD and a new idea for the treatment of VaD.

There were some limitations in the present study. First, VaD patients are mostly elderly, and the clinical manifestations of males and females are similar, while our study only used adolescent male rats. Therefore, factors such as gender and age need to be considered for further research. Secondly, while this study includes some cognitive assessments, it would be more convincing to add additional functional tests such as novel object recognition (NOR). More behavioral tests should be included in the future to verify the changes in cognitive function. Finally, this study mainly focused on the effects of TMAO on VaD neuroinflammation at the transcriptome level, and other potential protein interactions and pathways regulatory mechanisms need to be further explored in future research.

In summary, the present study elucidated, for the first time, that TMAO exacerbates neuroinflammation in VaD through the lncRNA Fendrr/miR-145-5p/PXN axis. Down-regulating Fendrr attenuates the VaD-induced cerebral injury via ceRNA interaction with miR-145-5p to suppress PXN expression. This offers a new insight into the mechanism of TMAO damage to VaD, which may facilitate a deeper comprehension of the pathological process of VaD and provide new options for clinical prevention or treatment.

Funding

This work was supported by the National Natural Science Foundation of China (82301609), China Postdoctoral Science Foundation (2022M711666), Natural Science Foundation of Jiangsu Province (BK20220196), the Medical Science and Technology Program of Nanjing (JQX20007), and Xinghuo Talent Program of Nanjing First Hospital.

Disclosure

This paper has been uploaded to ResearchSquare as a preprint: https://www.researchsquare.com/article/rs-3999274/v1. The authors report no conflicts of interest in this work.

References

1. Lourida I, Soni M, Thompson-Coon J, et al. Mediterranean diet, cognitive function, and dementia: a systematic review. *Epidemiology*. 2013;24(4):479–489. doi:10.1097/EDE.0b013e3182944410
2. World Health Organization. *Dementia: A Public Health Priority*. World Health Organization; 2012.
3. Farooq MU, Min J, Goshgarian C, Gorelick PB. Pharmacotherapy for vascular cognitive impairment. *CNS Drugs*. 2017;31(9):759–776. doi:10.1007/s40263-017-0459-3
4. Mulugeta E, Molina-Holgado F, Elliott MS, et al. Inflammatory mediators in the frontal lobe of patients with mixed and vascular dementia. *Dement Geriatr Cogn Disord*. 2008;25(3):278–286. doi:10.1159/000118633
5. Wang XX, Zhang B, Xia R, Jia QY. Inflammation, apoptosis and autophagy as critical players in vascular dementia. *Eur Rev Med Pharmacol Sci*. 2020;24(18):9601–9614.
6. Sun P, Su L, Zhu H, et al. Gut microbiota regulation and their implication in the development of neurodegenerative disease. *Microorganisms*. 2021;9(11):2281. doi:10.3390/microorganisms9112281
7. Alkasir R, Li J, Li X, Jin M, Zhu B. Human gut microbiota: the links with dementia development. *Protein Cell*. 2017;8(2):90–102. doi:10.1007/s13238-016-0338-6
8. Liu J, Sun J, Wang F, et al. Neuroprotective effects of clostridium butyricum against vascular dementia in mice via metabolic butyrate. *Biomed Res Int*. 2015;2015:412946.
9. Chen Y, Weng Z, Liu Q, et al. FMO3 and its metabolite TMAO contribute to the formation of gallstones. *Biochim Biophys Acta Mol Basis Dis*. 2019;1865(10):2576–2585.
10. Gao Q, Wang Y, Wang X, et al. Decreased levels of circulating trimethylamine N-oxide alleviate cognitive and pathological deterioration in transgenic mice: a potential therapeutic approach for Alzheimer's disease. *Aging*. 2019;11(19):8642–8663. doi:10.18632/aging.102352
11. Lanz M, Janeiro MH, Milagro FI, et al. Trimethylamine N-oxide (TMAO) drives insulin resistance and cognitive deficiencies in a senescence accelerated mouse model. *Mech Ageing Dev*. 2022;204:111668. doi:10.1016/j.mad.2022.111668
12. Wu C, Xue F, Lian Y, et al. Relationship between elevated plasma trimethylamine N-oxide levels and increased stroke injury. *Neurology*. 2020;94(7):e667–e677. doi:10.1212/WNL.0000000000008862
13. Li D, Ke Y, Zhan R, et al. Trimethylamine-N-oxide promotes brain aging and cognitive impairment in mice. *Aging Cell*. 2018;17(4):e12768. doi:10.1111/acel.12768
14. Deng Y, Zou J, Hong Y, et al. Higher circulating trimethylamine N-oxide aggravates cognitive impairment probably via downregulating hippocampal SIRT1 in vascular dementia rats. *Cells*. 2022;11(22):3650. doi:10.3390/cells11223650
15. Statello L, Guo CJ, Chen LL, Huarte M. Gene regulation by long non-coding RNAs and its biological functions. *Nat Rev Mol Cell Biol*. 2021;22(2):96–118.
16. Carelli S, Giallongo T, Rey F, et al. HuR interacts with lincBRN1a and lincBRN1b during neuronal stem cells differentiation. *RNA Biol*. 2019;16(10):1471–1485. doi:10.1080/15476286.2019.1637698
17. Chen SQ, Cai Q, Shen YY, Wang PY, Li MH, Teng GY. Neural stem cell transplantation improves spatial learning and memory via neuronal regeneration in amyloid-β precursor protein/presenilin 1/tau triple transgenic mice. *Am J Alzheimers Dis Other Demen*. 2014;29(2):142–149. doi:10.1177/1533317513506776

18. Dong B, Zhou B, Sun Z, et al. LncRNA-FENDRR mediates VEGFA to promote the apoptosis of brain microvascular endothelial cells via regulating miR-126 in mice with hypertensive intracerebral hemorrhage. *Microcirculation*. 2018;25(8):e12499. doi:10.1111/micc.12499
19. Wang L-Q, Zheng -Y-Y, Zhou H-J, Zhang -X-X, Wu P, Zhu S-M. LncRNA-Fendrr protects against the ubiquitination and degradation of NLRC4 protein through HERC2 to regulate the pyroptosis of microglia. *Mol Med*. 2021;27(1):39. doi:10.1186/s10020-021-00299-y
20. Gong C, Zhou X, Lai S, Wang L, Liu J. Long noncoding RNA/circular RNA-miRNA-mRNA axes in ischemia-reperfusion injury. *Biomed Res Int*. 2020;2020:8838524. doi:10.1155/2020/8838524
21. Cheng Y, Liu C, Liu Y, et al. Immune microenvironment related competitive endogenous RNA network as powerful predictors for melanoma prognosis based on WGCNA analysis. *Front Oncol*. 2020;10:577072. doi:10.3389/fonc.2020.577072
22. Yao ZH, Wang J, Shen BZ, et al. Identification of a hippocampal lncRNA-regulating network in cognitive dysfunction caused by chronic cerebral hypoperfusion. *Aging*. 2020;12(19):19520–19538. doi:10.18632/aging.103901
23. Zhao K, Zeng L, Cai Z, et al. RNA sequencing-based identification of the regulatory mechanism of microRNAs, transcription factors, and corresponding target genes involved in vascular dementia. *Front Neurosci*. 2022;16:917489. doi:10.3389/fnins.2022.917489
24. Tan L, Liu L, Yao J, Piao C. miR-145-5p attenuates inflammatory response and apoptosis in myocardial ischemia-reperfusion injury by inhibiting (NADPH) oxidase homolog 1. *Exp Anim*. 2021;70(3):311–321. doi:10.1538/expanim.20-0160
25. Yuan M, Zhang L, You F, et al. MiR-145-5p regulates hypoxia-induced inflammatory response and apoptosis in cardiomyocytes by targeting CD40. *Mol Cell Biochem*. 2017;431(1–2):123–131. doi:10.1007/s11010-017-2982-4
26. Yang W, Yang Y, Wan S, et al. Exploring the mechanism of the miRNA-145/paxillin axis in cell metabolism during VEGF-A-induced corneal angiogenesis. *Invest Ophthalmol Visual Sci*. 2021;62(10):25. doi:10.1167/iovs.62.10.25
27. Liu W, Huang X, Luo W, Liu X, Chen W. The role of paxillin aberrant expression in cancer and its potential as a target for cancer therapy. *Int J Mol Sci*. 2023;24(9):8245.
28. Alpha KM, Xu W, Turner CE. Paxillin family of focal adhesion adaptor proteins and regulation of cancer cell invasion. *Int Rev Cell Mol Biol*. 2020;355:1–52.
29. López-Colomé AM, Lee-Rivera I, Benavides-Hidalgo R, López E. Paxillin: a crossroad in pathological cell migration. *J Hematol Oncol*. 2017;10(1):50. doi:10.1186/s13045-017-0418-y
30. Yang Y, Ju J, Deng M, et al. Hypoxia inducible factor 1α promotes endogenous adaptive response in rat model of chronic cerebral hypoperfusion. *Int J Mol Sci*. 2017;18(1):3.
31. Euler M, Hoffmann MH. The double-edged role of neutrophil extracellular traps in inflammation. *Biochem Soc Trans*. 2019;47(6):1921–1930. doi:10.1042/BST20190629
32. Song Y, Wu Z, Zhao P. The protective effects of activating Sirt1/NF-κB pathway for neurological disorders. *Rev Neurosci*. 2022;33(4):427–438. doi:10.1515/revneuro-2021-0118
33. Fukata M, Vamadevan AS, Abreu MT. Toll-like receptors (TLRs) and Nod-like receptors (NLRs) in inflammatory disorders. *Semin Immunol*. 2009;21(4):242–253. doi:10.1016/j.smim.2009.06.005
34. Zhao S-P, Yu C, Yang M-S, Liu Z-L, Yang B-C, Xiao X-F. Long non-coding RNA FENDRR modulates autophagy through epigenetic suppression of ATG7 via binding PRC2 in acute pancreatitis. *Inflammation*. 2021;44(3):999–1013. doi:10.1007/s10753-020-01395-7
35. Han D, Gao Q, Cao F. Long noncoding RNAs (LncRNAs) - the dawning of a new treatment for cardiac hypertrophy and heart failure. *Biochim Biophys Acta Mol Basis Dis*. 2017;1863(8):2078–2084. doi:10.1016/j.bbadis.2017.02.024
36. Lin W, Zhou Q, Wang C-Q, et al. LncRNAs regulate metabolism in cancer. *Int J Biol Sci*. 2020;16(7):1194–1206. doi:10.7150/ijbs.40769
37. Vasudeva K, Dutta A, Munshi A. Role of lncRNAs in the development of ischemic stroke and their therapeutic potential. *Mol Neurobiol*. 2021;58(8):3712–3728. doi:10.1007/s12035-021-02359-0
38. Jiang Z, Zhang J. Mesenchymal stem cell-derived exosomes containing miR-145-5p reduce inflammation in spinal cord injury by regulating the TLR4/NF-κB signaling pathway. *Cell Cycle*. 2021;20(10):993–1009. doi:10.1080/15384101.2021.1919825
39. Fang C, Li Q, Min G, et al. MicroRNA-181c ameliorates cognitive impairment induced by chronic cerebral hypoperfusion in rats. *Mol Neurobiol*. 2017;54(10):8370–8385. doi:10.1007/s12035-016-0268-6
40. Duncombe J, Kitamura A, Hase Y, Ihara M, Kalaria RN, Horsburgh K. Chronic cerebral hypoperfusion: a key mechanism leading to vascular cognitive impairment and dementia. Closing the translational gap between rodent models and human vascular cognitive impairment and dementia. *Clin Sci*. 2017;131(19):2451–2468. doi:10.1042/CS20160727
41. Sha S, Tan J, Miao Y, Zhang Q. The role of autophagy in hypoxia-induced neuroinflammation. *DNA Cell Biol*. 2021;40(6):733–739. doi:10.1089/dna.2020.6186
42. Belkhelfa M, Beder N, Mouhoub D, et al. The involvement of neuroinflammation and necroptosis in the hippocampus during vascular dementia. *J Neuroimmunol*. 2018;320:48–57. doi:10.1016/j.jneuroim.2018.04.004
43. Tian Z, Ji X, Liu J. Neuroinflammation in vascular cognitive impairment and dementia: current evidence, advances, and prospects. *Int J Mol Sci*. 2022;23(11):6224. doi:10.3390/ijms23116224
44. Venkat P, Chopp M, Chen J. Models and mechanisms of vascular dementia. *Exp Neurol*. 2015;272:97–108. doi:10.1016/j.expneurol.2015.05.006
45. Farkas E, Luiten PG, Bari F. Permanent, bilateral common carotid artery occlusion in the rat: a model for chronic cerebral hypoperfusion-related neurodegenerative diseases. *Brain Res Rev*. 2007;54(1):162–180. doi:10.1016/j.brainresrev.2007.01.003
46. Zheng C, Yang C, Gao D, et al. Cornel iridoid glycoside alleviates microglia-mediated inflammatory response via the NLRP3/calpain pathway. *J Agric Food Chem*. 2022;70(38):11967–11980. doi:10.1021/acs.jafc.2c03851
47. Shamaa OR. *Intracellular and Extracellular Regulation of the Inflammatory Protease Caspase-1*. The Ohio State University; 2014.
48. Cheng YC, Chu LW, Chen JY, et al. Loganin attenuates high glucose-induced Schwann cells pyroptosis by inhibiting ROS generation and NLRP3 inflammasome activation. *Cells*. 2020;9(9):1948. doi:10.3390/cells9091948
49. Zhang Y, Zhang C, Li H, Hou J. The presence of high levels of circulating trimethylamine N-oxide exacerbates central and peripheral inflammation and inflammatory hyperalgesia in rats following carrageenan injection. *Inflammation*. 2019;42(6):2257–2266. doi:10.1007/s10753-019-01090-2
50. Chen H, Li J, Li N, Liu H, Tang J. Increased circulating trimethylamine N-oxide plays a contributory role in the development of endothelial dysfunction and hypertension in the RUPP rat model of preeclampsia. *Hypertens Pregnancy*. 2019;38(2):96–104. doi:10.1080/10641955.2019.1584630

51. Liu A, Zhang Y, Xun S, Sun M. Trimethylamine N-oxide promotes atherosclerosis via regulating the enriched abundant transcript 1/miR-370-3p/signal transducer and activator of transcription 3/flavin-containing monooxygenase-3 axis. *Bioengineered*. 2022;13(1):1541–1553. doi:10.1080/21655979.2021.2010312
52. Wang P, Mao S, Yi T, Wang L. LncRNA MALAT1 targets miR-9-3p to upregulate SAP97 in the hippocampus of mice with vascular dementia. *Biochem Genet*. 2023;61(3):916–930. doi:10.1007/s10528-022-10289-2
53. Yue D, Guanqun G, Jingxin L, et al. Silencing of long noncoding RNA XIST attenuated Alzheimer's disease-related BACE1 alteration through miR-124. *Cell Biol Int*. 2020;44(2):630–636. doi:10.1002/cbin.11263
54. Zhang G, Han G, Zhang X, et al. Long non-coding RNA FENDRR reduces prostate cancer malignancy by competitively binding miR-18a-5p with RUNX1. *Biomarkers*. 2018;23(5):435–445. doi:10.1080/1354750X.2018.1443509
55. He W, Zhong G, Wang P, Jiang C, Jiang N, Huang J. Downregulation of long noncoding RNA FENDRR predicts poor prognosis in renal cell carcinoma. *Oncol Lett*. 2019;17(1):103–112.
56. Zhu Y, Zhang X, Wang L, et al. FENDRR suppresses cervical cancer proliferation and invasion by targeting miR-15a/b-5p and regulating TUBA1A expression. *Cancer Cell Int*. 2020;20:152. doi:10.1186/s12935-020-01223-w
57. Ang CE, Trevino AE, Chang HY. Diverse lncRNA mechanisms in brain development and disease. *Curr Opin Genet Dev*. 2020;65:42–46. doi:10.1016/j.gde.2020.05.006
58. Qi X, Shao M, Sun H, Shen Y, Meng D, Huo W. Long non-coding RNA SNHG14 promotes microglia activation by regulating miR-145-5p/PLA2G4A in cerebral infarction. *Neuroscience*. 2017;348:98–106.
59. Liang C, Wang S, Zhao L, Han Y, Zhang M. Effects of miR-145-5p on cardiomyocyte proliferation and apoptosis, GIGYF1 expression and oxidative stress response in rats with myocardial ischemia-reperfusion. *Cell Mol Biol*. 2022;68(1):147–159. doi:10.14715/cmb/2022.68.1.19
60. Christopher E. Molecules in focus paxillin. *Int J Biochem Cell B*. 1998;30(9):959.
61. Lin K-H, Kumar VB, Shanmugam T, et al. miR-145-5p targets paxillin to attenuate angiotensin II-induced pathological cardiac hypertrophy via downregulation of Rac 1, pJNK, p-c-Jun, NFATc3, ANP and by Sirt-1 upregulation. *Mol Cell Biochem*. 2021;476(9):3253–3260. doi:10.1007/s11010-021-04100-w
62. Qin J, Wang F, Jiang H, Xu J, Jiang Y, Wang Z. MicroRNA-145 suppresses cell migration and invasion by targeting paxillin in human colorectal cancer cells. *Int J Clin Exp Pathol*. 2015;8(2):1328–1340.
63. Wang W, Hu D, Feng Y, et al. Paxillin mediates ATP-induced activation of P2X7 receptor and NLRP3 inflammasome. *BMC Biol*. 2020;18(1):182. doi:10.1186/s12915-020-00918-w
64. Erdö F, Trapp T, Mies G, Hossmann K-A. Immunohistochemical analysis of protein expression after middle cerebral artery occlusion in mice. *Acta Neuropathol*. 2004;107(2):127–136. doi:10.1007/s00401-003-0789-8
65. Liu J, Zhou C-X, Zhang Z-J, Wang L-Y, Jing Z-W, Wang Z. Synergistic mechanism of gene expression and pathways between jasminoidin and ursodeoxycholic acid in treating focal cerebral ischemia-reperfusion injury. *CNS Neurosci Ther*. 2012;18(8):674–682. doi:10.1111/j.1755-5949.2012.00348.x